Supporting Information

Mechanistic insight into inhibition of two-component system signaling

Samson Francis,[a] Kaelyn E. Wilke,[a] Douglas E. Brown[a] and Erin E. Carlson[a,b*]

[a] Department of Chemistry, Indiana University, 800 E. Kirkwood Avenue, Bloomington, Indiana, USA.
[b] Department of Molecular and Cellular Biochemistry, Indiana University, 212 S. Hawthorne Drive, Bloomington, Indiana, USA.
Corresponding Author: carlsone@indiana.edu

Contents

Supporting Information Figures and Tables

Table S1. Rank and score of compounds reported to demonstrate TCS inhibitory activities and their corresponding Surflex score, rank, and documented biological data.

#	Structure	Receptor 1ID0		Receptor 1I58		Receptor 2C2A		Receptor 3CGY						
		Surflex Score	Rank	Surflex Score	Rank	Surflex Score	Rank	Surflex Score	Rank	TCS Tested	IC_{50} HK (μM)	IC_{50} RR (μM)	MIC	Ref.
1	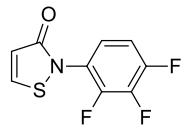	2.6341	1029	3.251	1030	3.5142	1040	3.0847	953	AlgR2	2	-	-	[1]
2	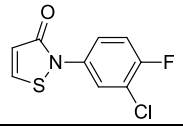	3.0404	1009	3.518	1018	3.8778	1029	1.6857	1040	AlgR2	2	-	-	[1]
3	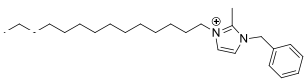	5.2403	559	8.7544	79	9.2257	141	6.3868	126	AlgR1 AlgR2 CheA NR_{II} KinA	0.4-0.6	-	-	[1]
4	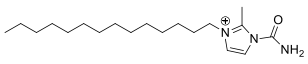	7.868	52	9.8076	23	8.7226	212	5.6508	278	AlgR1 AlgR2 CheA NR_{II} KinA	0.4-0.6	-	-	[1]
5	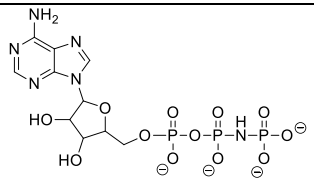	9.8154	6	8.2835	132	9.2701	143	6.8504	75	HpKA-DrrA	-	-	-	[2]
6	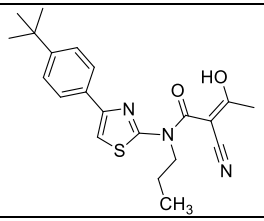	4.4319	808	3.7157	1002	5.0129	984	2.6174	1005	HpKA-DrrA	30	30	1	[2]

7	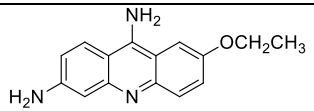	6.1823	311	6.2405	533	7.7782	412	5.3572	353	HpKA-DrrA	29.5	29.5	-	[2]
8	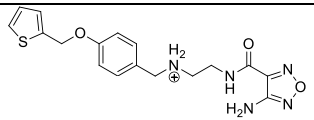	5.3822	522	6.9377	373	9.3379	128	5.6119	276	VicK	542.3	-	100	[3]
9	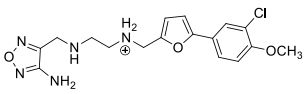	7.8251	58	7.6137	231	9.078	159	5.9994	192	VicK	562.4	-	50	[3]
10	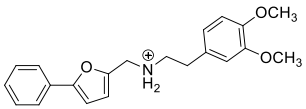	6.0155	357	8.5172	101	10.0246	58	5.3371	359	VicK	502.6	-	100	[3]
11	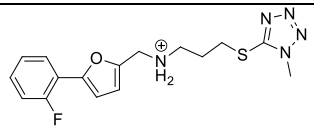	6.0603	342	7.1185	334	8.4564	268	5.8769	214	VicK	>1000	-	100	[3]
12	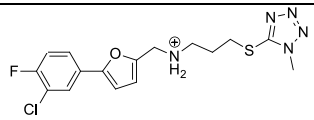	7.7916	61	7.3906	277	8.6092	234	5.7907	235	VicK	598.1	-	>1000	[3]
13	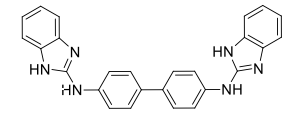	5.2888	546	4.6756	896	7.8139	405	4.9899	460	VicK	32.60	-	0.28	[3]
14	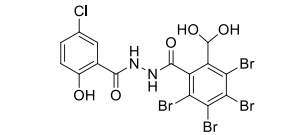	5.3948	516	3.9942	978	6.3423	786	4.4055	630	YycG	48	-	50	[4]
15	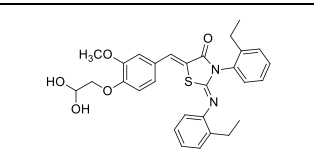	5.2857	547	8.0385	167	10.4673	31	5.1475	414	YycG	29	-	25	[4]

16	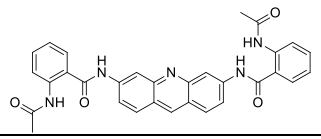	5.5479	478	6.6358	439	6.5453	733	5.3259	366	YycG	15	-	12.5	[4]
17	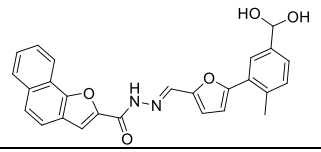	7.6617	73	7.7787	203	11.8361	4	6.8505	74	YycG	13.5	-	12.5	[4]
18	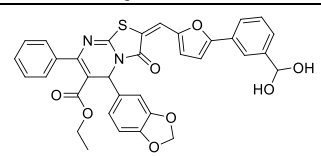	7.0096	157	7.7609	207	10.9232	16	7.8013	14	YycG	14	-	6.25	[4]
19	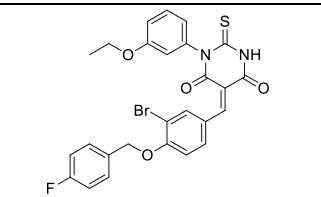	5.3834	521	4.8536	844	6.5453	733	4.3176	665	YycG	>200	-	100	[4]
20	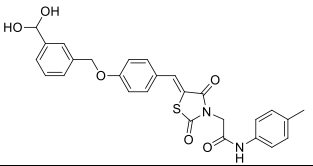	7.1043	134	8.9119	64	10.6944	21	5.863	220	YycG	6.5	-	0.2	[4]
21	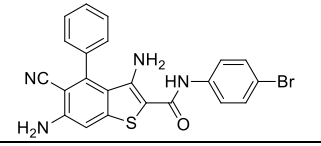	6.2702	292	7.1734	324	4.793	1002	4.787	515	HpKA-DrrA	0.41	-	-	[5]
22	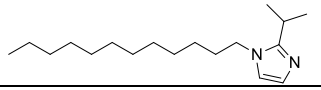	7.0299	153	8.2833	133	8.9824	171	4.1039	737	YycG	76.5	-	25	[6]

23	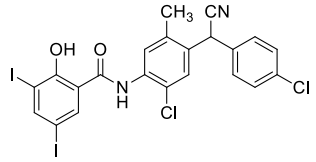	3.0818	1006	4.2318	953	6.3662	779	4.0584	750	KinA-Spo0F	3.8	3.8	1	[7, 8]
24	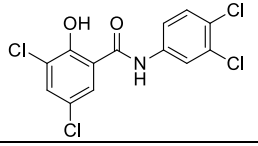	2.911	1017	1.7244	1045	4.4539	1019	3.8547	805	KinA-Spo0F	45	45	0.5	[8]
25	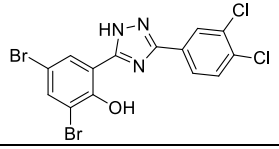	4.3917	823	4.9325	832	4.9996	986	4.3085	667	KinA-Spo0F	25	25	0.25-1	[9]
26	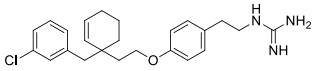	8.6015	23	9.6129	30	10.2441	46	8.0292	8	KinA-Spo0F NR_{II} -NR_{I}	18	17	2	
27	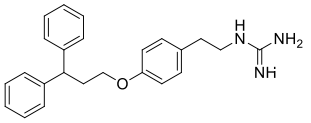	8.4203	28	9.6948	26	9.8122	75	7.329	41	KinA-Spo0F	20	20	1-8	[10]
28	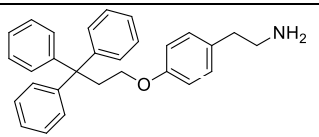	7.1628	120	8.1661	150	8.7985	201	5.3119	371	KinA-Spo0F	14	14	2-16	[10]
29	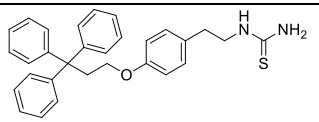	7.3131	105	9.7372	24	10.1496	50	8.5535	4	KinA-Spo0F	500	500	>32	[10]
30	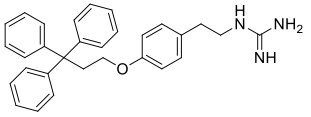	8.8116	17	11.9226	1	10.1188	51	8.0015	10	KinA-Spo0F	1.6	1.6	1-2	[7, 10]

31	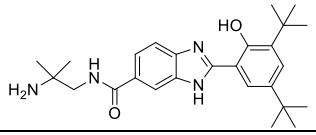	2.0797	1041	5.9444	605	7.6126	453	3.7753	824	KinA-NR_{II}	10	13	2	[7]
32	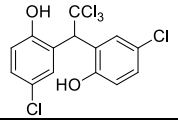	2.8973	1018	2.4744	1043	3.8343	1033	3.5477	871	KinA-NR_{II}	4	23	2	[7]
33	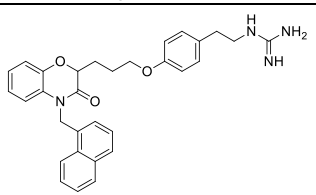	9.1179	15	11.8906	2	12.2995	2	7.9565	12	KinA-NR_{II}	13	37	1-2	[7]
34	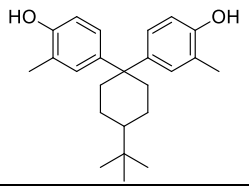	7.1542	122	7.7735	206	7.1523	570	6.3414	135	KinA-NR_{II}	-	-	1-2	[11]
35	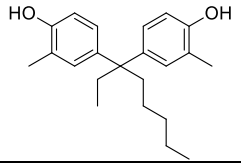	5.7593	419	6.5629	463	7.4925	479	6.5575	109	KinA-NR_{II}	1.6	1.6	2-4	[11]
36	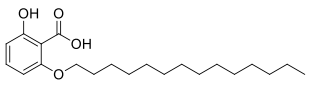	9.675	8	8.4989	103	10.0395	57	5.4886	317	NR_I-NR_{II} KinA-Spo0F	2.2 KinA-Spo0F	5.0 NR_I-NR_{II}	4.0	[12]
37	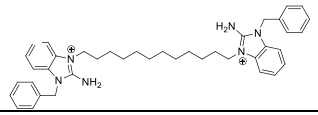	6.1775	314	7.6961	218	10.9788	15	6.7903	80	HprK/P	-	-	-	[13]
38	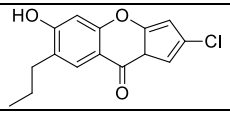	4.0165	896	5.0779	797	6.0328	845	3.5474	872	NR_{II}	20	1.6	0.78	[14]

41	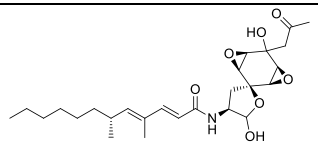	10.6889	2	9.8774	21	10.2665	43	6.2297	159	YycF-YycG	211-232	-	15.3	[15]
42	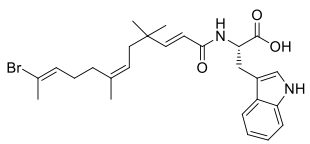	8.1599	37	7.6784	221	10.0723	54	5.9517	197	YycF-YycG	43.9	-	25	[16]
43	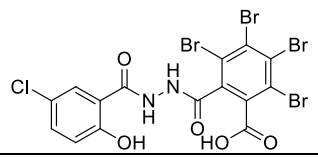	2.5472	1031	3.3949	1026	5.8565	876	5.0749	431	SF-EnvZc	70.17	70.17	12.5	[11]
44	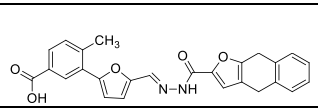	5.5586	475	6.5012	479	9.15	147	4.2241	695	SF-EnvZc	10.18	10.18	12.5	[11]
45	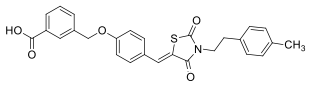	6.5939	222	8.2712	136	10.0048	60	5.1254	418	SF-EnvZc	10.2	10.2	-	[11]
46	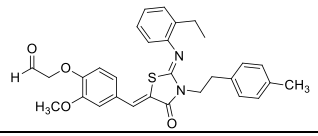	6.2265	301	6.1311	558	9.9799	63	4.8146	500	YycF-YycG	-	-	25-100	[17]
47	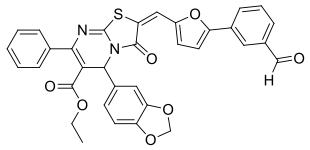	6.501	241	8.0366	168	8.331	295	5.7463	251	YycF-YycG	-	-	25-100	[17]

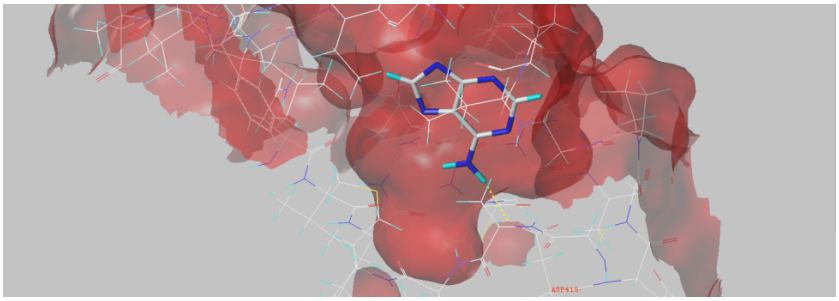

Fig. S1 The fragment-guided docking approach in Surflex. A portion of the co-crystallized ligand (shown with the adenine moiety in the receptor PhoQ, PDB: 1ID0) is retained and utilized to guide the placement of compounds in the active site.

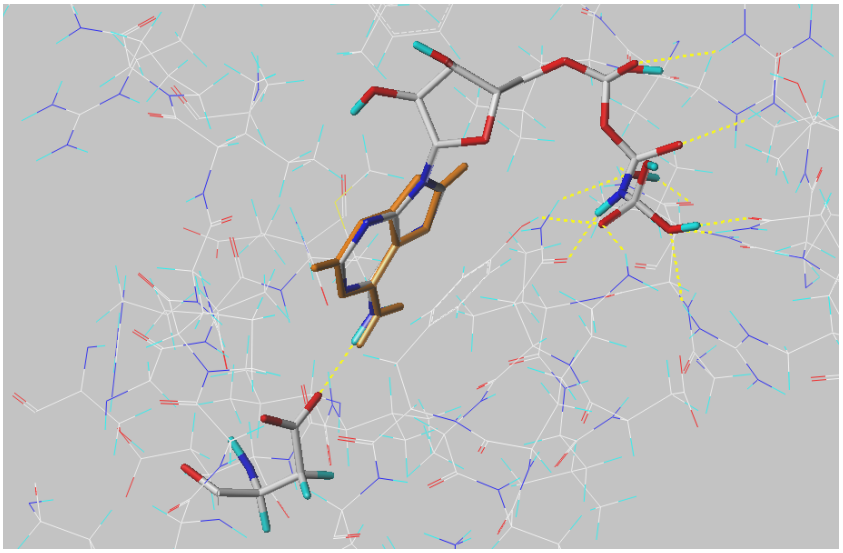

Fig. S2 The docked conformation of AMP-PNP in the active site of PhoQ superimposed with the adenine moiety (orange) of the co-crystallized structure. The computed RMSD between these two moieties was 0.108.

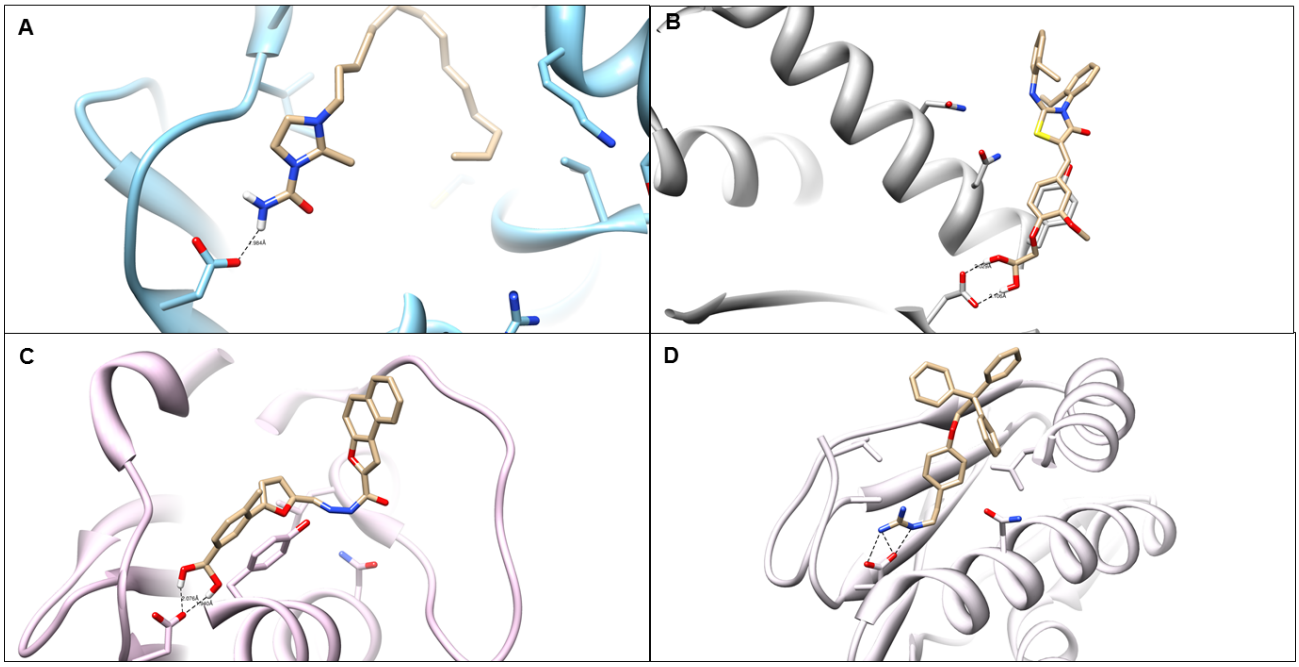

Fig. S3 Predicted binding poses of selected TCS inhibitors in the nucleotide-binding region of HKs. Some portions of the protein have been cut away for clarity. (A) Compound **4** interacting with Asp449 in receptor 1I58. (B) The interaction of compound **15** with Asp411 in receptor 2C2A. (C) Asp415 interacting with inhibitor **20** in receptor 1ID0. (D) Salt-bridge interaction formed between inhibitor **30** and Asp416 of 3CGY.

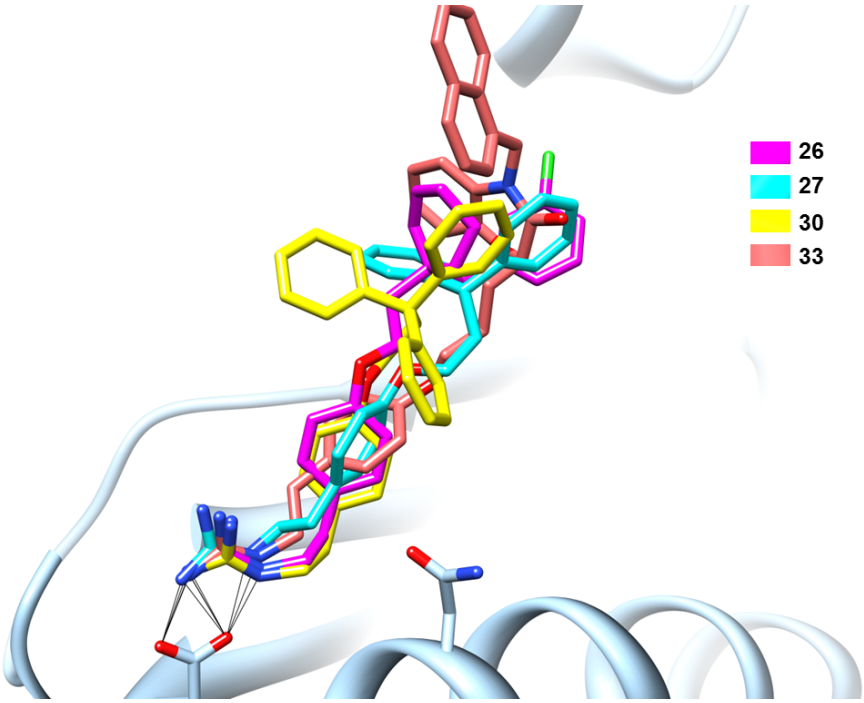

Fig. S4 Cluster of guanidine-bearing compounds (**26**, **27**, **30**, **33**) and their corresponding interactions with Asp416 of PhoQ (3CGY; *E. coli*).

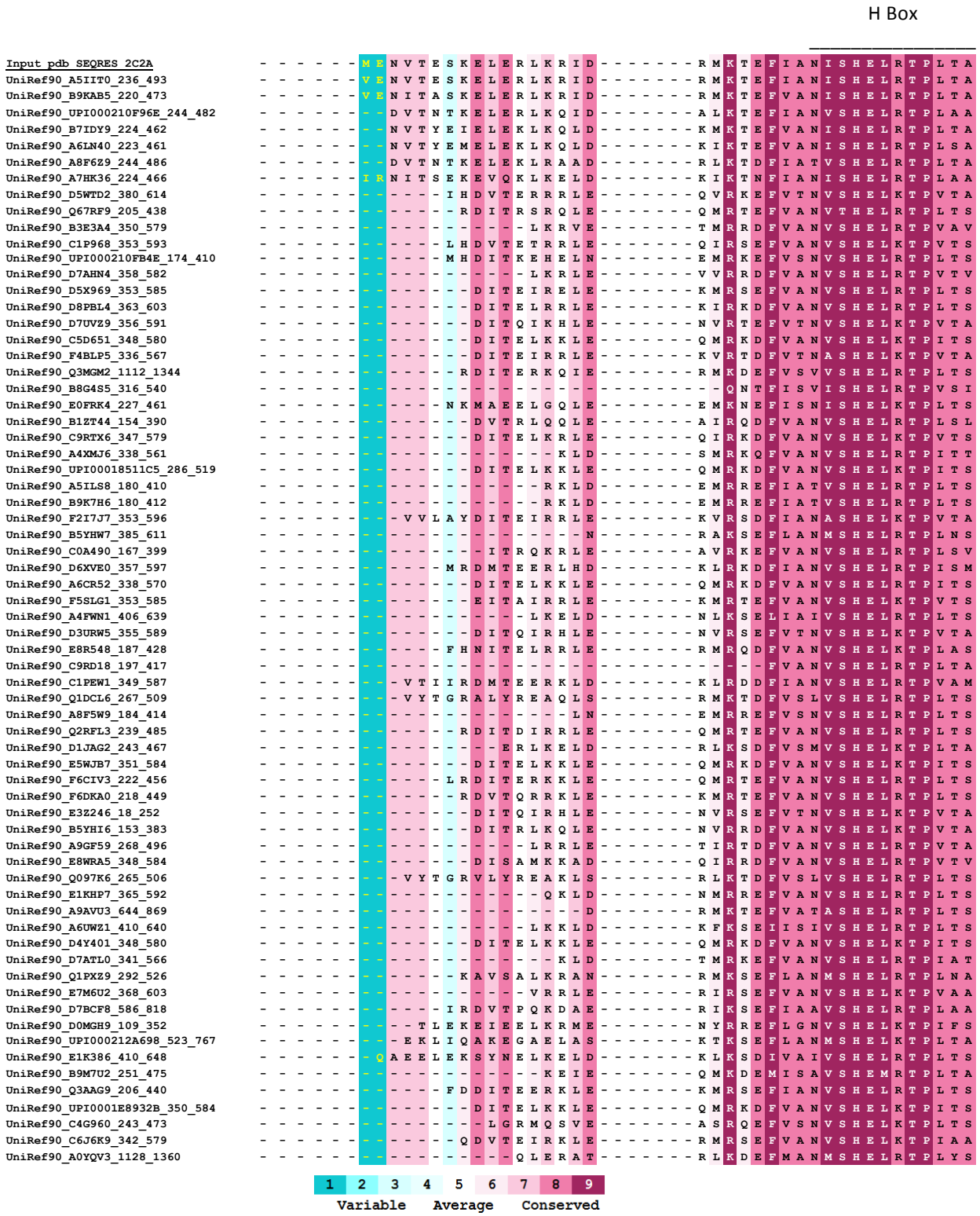

Fig. S5 The complete multiple sequence alignment (MSA) of HK homologs retrieved from the UniProt database and aligned using the Consurf Protein database.[18] Highly-conserved active site residues are outlined in red and indicated by a red arrow (Asn found in N Box region, Asp found in G1 box region, Leu found in G2 box).

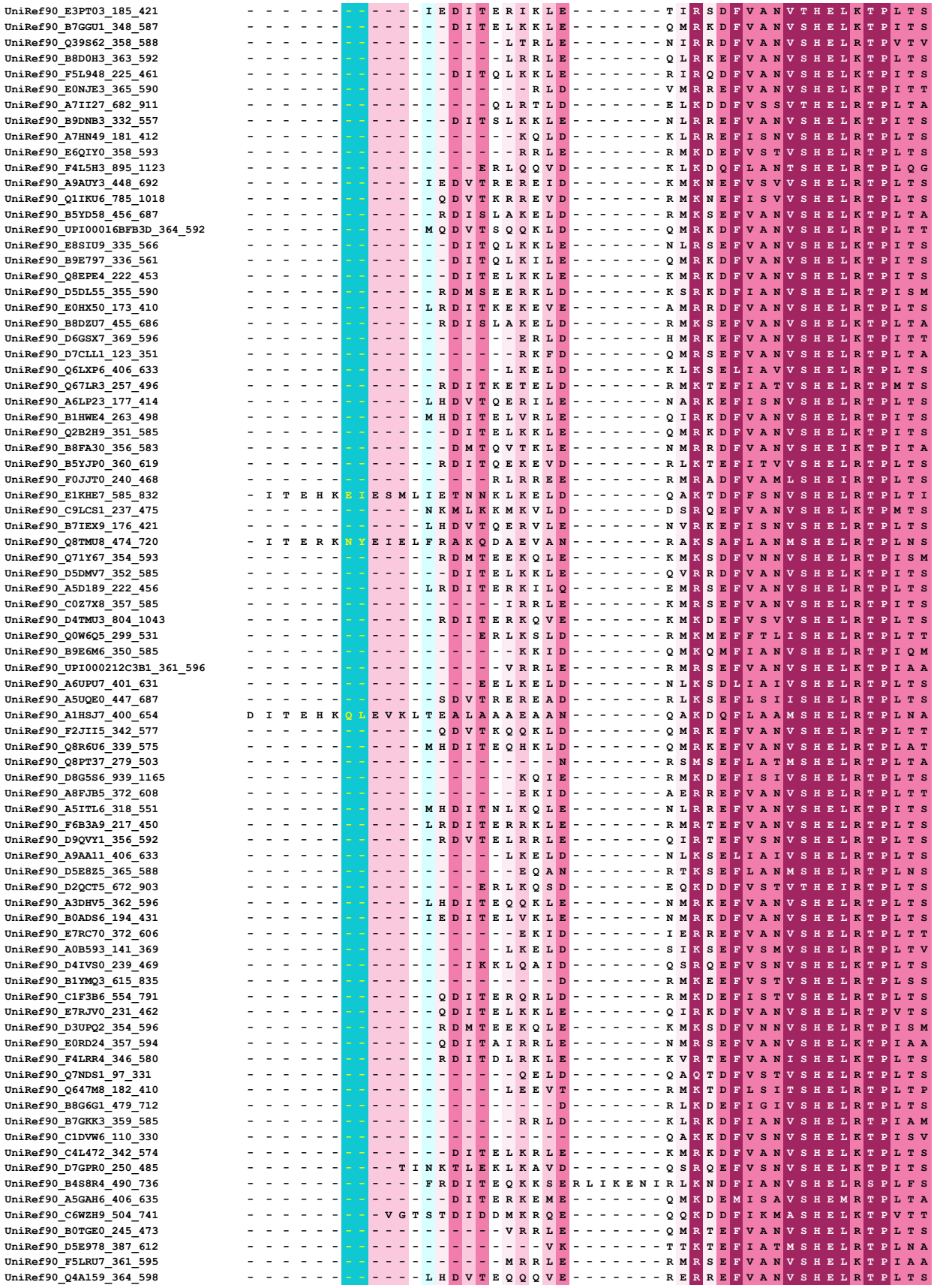
UniRef90_E3PT03_185_421
UniRef90_B7GGU1_348_587
UniRef90_Q39S62_358_588
UniRef90_B8D0H3_363_592
UniRef90_F5L948_225_461
UniRef90_E0NJE3_365_590
UniRef90_A7II27_682_911
UniRef90_B9DNB3_332_557
UniRef90_A7HN49_181_412
UniRef90_E6QIY0_358_593
UniRef90_F4L5H3_895_1123
UniRef90_A9AUY3_448_692
UniRef90_Q1IKU6_785_1018
UniRef90_B5YD58_456_687
UniRef90_UPI00016BFB3D_364_592
UniRef90_E8SIU9_335_566
UniRef90_B9E797_336_561
UniRef90_Q8EPE4_222_453
UniRef90_D5DL55_355_590
UniRef90_E0HX50_173_410
UniRef90_B8DZU7_455_686
UniRef90_D6GSX7_369_596
UniRef90_D7CLL1_123_351
UniRef90_Q6LXP6_406_633
UniRef90_Q67LR3_257_496
UniRef90_A6LP23_177_414
UniRef90_B1HWE4_263_498
UniRef90_Q2B2H9_351_585
UniRef90_B8FA30_356_583
UniRef90_B5YJP0_360_619
UniRef90_F0JJT0_240_468
UniRef90_E1KHE7_585_832
UniRef90_C9LCS1_237_475
UniRef90_B7IEX9_176_421
UniRef90_Q8TMU8_474_720
UniRef90_Q71Y67_354_593
UniRef90_D5DMV7_352_585
UniRef90_A5D189_222_456
UniRef90_C0Z7X8_357_585
UniRef90_D4TMU3_804_1043
UniRef90_Q0W6Q5_299_531
UniRef90_B9E6M6_350_585
UniRef90_UPI000212C3B1_361_596
UniRef90_A6UPU7_401_631
UniRef90_A5UQE0_447_687
UniRef90_A1HSJ7_400_654
UniRef90_F2JII5_342_577
UniRef90_Q8R6U6_339_575
UniRef90_Q8PT37_279_503
UniRef90_D8G5S6_939_1165
UniRef90_A8FJB5_372_608
UniRef90_A5ITL6_318_551
UniRef90_F6B3A9_217_450
UniRef90_D9QVY1_356_592
UniRef90_A9AA11_406_633
UniRef90_D5E8Z5_365_588
UniRef90_D2QCT5_672_903
UniRef90_A3DHV5_362_596
UniRef90_B0ADS6_194_431
UniRef90_E7RC70_372_606
UniRef90_A0B593_141_369
UniRef90_D4IVS0_239_469
UniRef90_B1YMQ3_615_835
UniRef90_C1F3B6_554_791
UniRef90_E7RJV0_231_462
UniRef90_D3UPQ2_354_596
UniRef90_E0RD24_357_594
UniRef90_F4LRR4_346_580
UniRef90_Q7NDS1_97_331
UniRef90_Q647M8_182_410
UniRef90_B8G6G1_479_712
UniRef90_B7GKK3_359_585
UniRef90_C1DVW6_110_330
UniRef90_C4L472_342_574
UniRef90_D7GPR0_250_485
UniRef90_B4S8R4_490_736
UniRef90_A5GAH6_406_635
UniRef90_C6WZH9_504_741
UniRef90_B0TGE0_245_473
UniRef90_D5E978_387_612
UniRef90_F5LRU7_361_595
UniRef90_Q4A159_364_598


H Box
Input pdb SEQRES 2C2A
UniRef90_A5IIT0_236_493
UniRef90_B9KAB5_220_473
UniRef90_UPI000210F96E_244_482
UniRef90_B7IDY9_224_462
UniRef90_A6LN40_223_461
UniRef90_A8F6Z9_244_486
UniRef90_A7HK36_224_466
UniRef90_D5WTD2_380_614
UniRef90_Q67RF9_205_438
UniRef90_B3E3A4_350_579
UniRef90_C1P968_353_593
UniRef90_UPI000210FB4E_174_410
UniRef90_D7AHN4_358_582
UniRef90_D5X969_353_585
UniRef90_D8PBL4_363_603
UniRef90_D7UVZ9_356_591
UniRef90_C5D651_348_580
UniRef90_F4BLP5_336_567
UniRef90_Q3MGM2_1112_1344
UniRef90_B8G4S5_316_540
UniRef90_E0FRK4_227_461
UniRef90_B1ZT44_154_390
UniRef90_C9RTX6_347_579
UniRef90_A4XMJ6_338_561
UniRef90_UPI00018511C5_286_519
UniRef90_A5ILS8_180_410
UniRef90_B9K7H6_180_412
UniRef90_F2I7J7_353_596
UniRef90_B5YHW7_385_611
UniRef90_C0A490_167_399
UniRef90_D6XVE0_357_597
UniRef90_A6CR52_338_570
UniRef90_F5SLG1_353_585
UniRef90_A4FWN1_406_639
UniRef90_D3URW5_355_589
UniRef90_E8R548_187_428
UniRef90_C9RD18_197_417
UniRef90_C1PEW1_349_587
UniRef90_Q1DCL6_267_509
UniRef90_A8F5W9_184_414
UniRef90_Q2RFL3_239_485
UniRef90_D1JAG2_243_467
UniRef90_E5WJB7_351_584
UniRef90_F6CIV3_222_456
UniRef90_F6DKA0_218_449
UniRef90_E3Z246_18_252
UniRef90_B5YHI6_153_383
UniRef90_A9GF59_268_496
UniRef90_E8WRA5_348_584
UniRef90_Q097K6_265_506
UniRef90_E1KHP7_365_592
UniRef90_A9AVU3_644_869
UniRef90_A6UWZ1_410_640
UniRef90_D4Y401_348_580
UniRef90_D7ATL0_341_566
UniRef90_Q1PXZ9_292_526
UniRef90_E7M6U2_368_603
UniRef90_D7BCF8_586_818
UniRef90_D0MGH9_109_352
UniRef90_UPI000212A698_523_767
UniRef90_E1K386_410_648
UniRef90_B9M7U2_251_475
UniRef90_Q3AAG9_206_440
UniRef90_UPI0001E8932B_350_584
UniRef90_C4G960_243_473
UniRef90_C6J6K9_342_579
UniRef90_A0YQV3_1128_1360

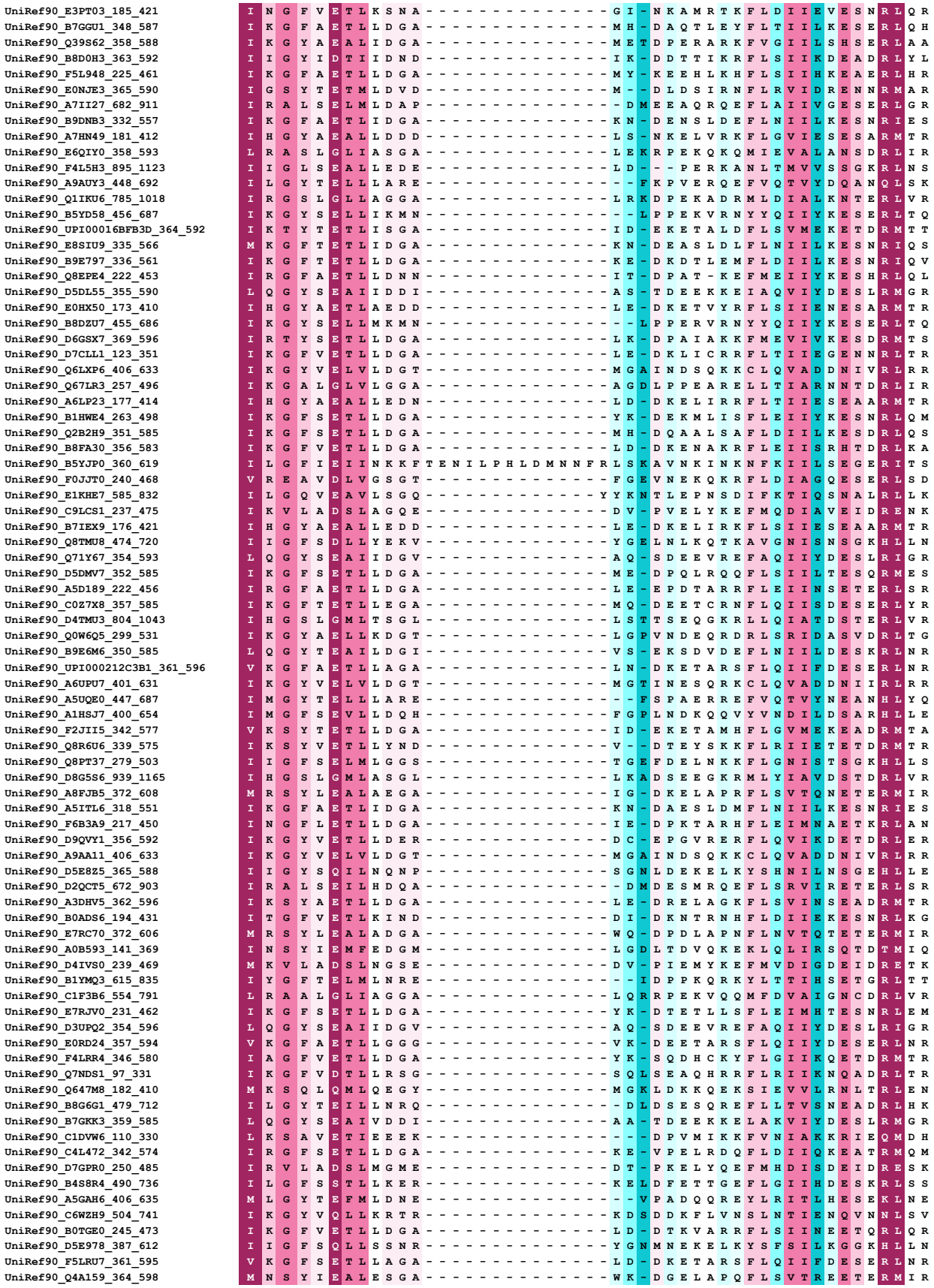
UniRef90_E3PT03_185_421
UniRef90_B7GGU1_348_587
UniRef90_Q39S62_358_588
UniRef90_B8D0H3_363_592
UniRef90_F5L948_225_461
UniRef90_E0NJE3_365_590
UniRef90_A7II27_682_911
UniRef90_B9DNB3_332_557
UniRef90_A7HN49_181_412
UniRef90_E6QIY0_358_593
UniRef90_F4L5H3_895_1123
UniRef90_A9AUY3_448_692
UniRef90_Q1IKU6_785_1018
UniRef90_B5YD58_456_687
UniRef90_UPI00016BFB3D_364_592
UniRef90_E8SIU9_335_566
UniRef90_B9E797_336_561
UniRef90_Q8EPE4_222_453
UniRef90_D5DL55_355_590
UniRef90_E0HX50_173_410
UniRef90_B8DZU7_455_686
UniRef90_D6GSX7_369_596
UniRef90_D7CLL1_123_351
UniRef90_Q6LXP6_406_633
UniRef90_Q67LR3_257_496
UniRef90_A6LP23_177_414
UniRef90_B1HWE4_263_498
UniRef90_Q2B2H9_351_585
UniRef90_B8FA30_356_583
UniRef90_B5YJP0_360_619
UniRef90_F0JJT0_240_468
UniRef90_E1KHE7_585_832
UniRef90_C9LCS1_237_475
UniRef90_B7IEX9_176_421
UniRef90_Q8TMU8_474_720
UniRef90_Q71Y67_354_593
UniRef90_D5DMV7_352_585
UniRef90_A5D189_222_456
UniRef90_C0Z7X8_357_585
UniRef90_D4TMU3_804_1043
UniRef90_Q0W6Q5_299_531
UniRef90_B9E6M6_350_585
UniRef90_UPI000212C3B1_361_596
UniRef90_A6UPU7_401_631
UniRef90_A5UQE0_447_687
UniRef90_A1HSJ7_400_654
UniRef90_F2JII5_342_577
UniRef90_Q8R6U6_339_575
UniRef90_Q8PT37_279_503
UniRef90_D8G5S6_939_1165
UniRef90_A8FJB5_372_608
UniRef90_A5ITL6_318_551
UniRef90_F6B3A9_217_450
UniRef90_D9QVY1_356_592
UniRef90_A9AA11_406_633
UniRef90_D5E8Z5_365_588
UniRef90_D2QCT5_672_903
UniRef90_A3DHV5_362_596
UniRef90_B0ADS6_194_431
UniRef90_E7RC70_372_606
UniRef90_A0B593_141_369
UniRef90_D4IVS0_239_469
UniRef90_B1YMQ3_615_835
UniRef90_C1F3B6_554_791
UniRef90_E7RJV0_231_462
UniRef90_D3UPQ2_354_596
UniRef90_E0RD24_357_594
UniRef90_F4LRR4_346_580
UniRef90_Q7NDS1_97_331
UniRef90_Q647M8_182_410
UniRef90_B8G6G1_479_712
UniRef90_B7GKK3_359_585
UniRef90_C1DVW6_110_330
UniRef90_C4L472_342_574
UniRef90_D7GPR0_250_485
UniRef90_B4S8R4_490_736
UniRef90_A5GAH6_406_635
UniRef90_C6WZH9_504_741
UniRef90_B0TGE0_245_473
UniRef90_D5E978_387_612
UniRef90_F5LRU7_361_595
UniRef90_Q4A159_364_598

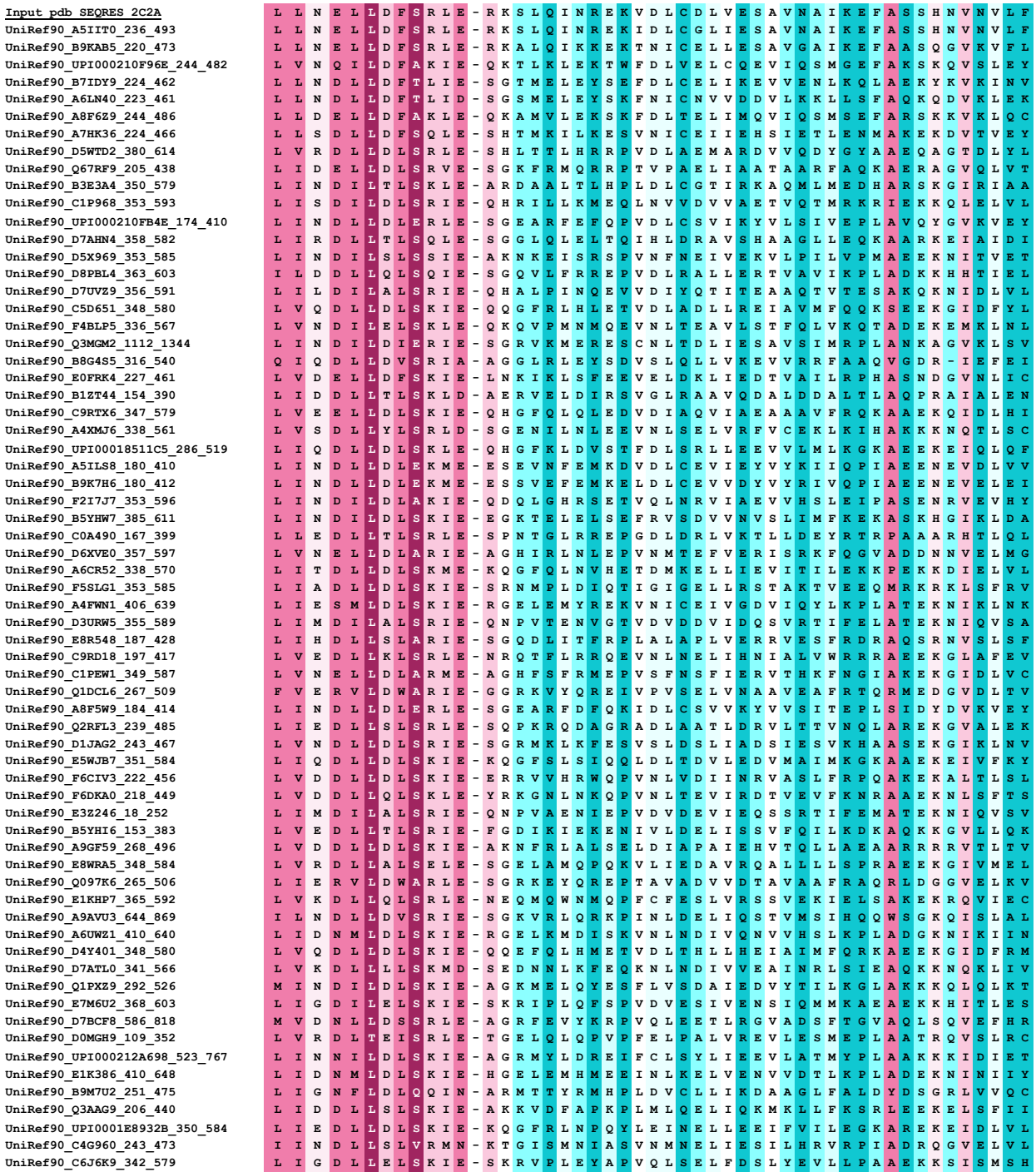
Input_pdb_SEQRES_2C2A
UniRef90_A5IIT0_236_493
UniRef90_B9KAB5_220_473
UniRef90_UPI000210F96E_244_482
UniRef90_B7IDY9_224_462
UniRef90_A6LN40_223_461
UniRef90_A8F6Z9_244_486
UniRef90_A7HK36_224_466
UniRef90_D5WTD2_380_614
UniRef90_Q67RF9_205_438
UniRef90_B3E3A4_350_579
UniRef90_C1P968_353_593
UniRef90_UPI000210FB4E_174_410
UniRef90_D7AHN4_358_582
UniRef90_D5X969_353_585
UniRef90_D8PBL4_363_603
UniRef90_D7UVZ9_356_591
UniRef90_C5D651_348_580
UniRef90_F4BLP5_336_567
UniRef90_Q3MGM2_1112_1344
UniRef90_B8G4S5_316_540
UniRef90_E0FRK4_227_461
UniRef90_B1ZT44_154_390
UniRef90_C9RTX6_347_579
UniRef90_A4XMJ6_338_561
UniRef90_UPI00018511C5_286_519
UniRef90_A5ILS8_180_410
UniRef90_B9K7H6_180_412
UniRef90_F2I7J7_353_596
UniRef90_B5YHW7_385_611
UniRef90_C0A490_167_399
UniRef90_D6XVE0_357_597
UniRef90_A6CR52_338_570
UniRef90_F5SLG1_353_585
UniRef90_A4FWN1_406_639
UniRef90_D3URW5_355_589
UniRef90_E8R548_187_428
UniRef90_C9RD18_197_417
UniRef90_C1PEW1_349_587
UniRef90_Q1DCL6_267_509
UniRef90_A8F5W9_184_414
UniRef90_Q2RFL3_239_485
UniRef90_D1JAG2_243_467
UniRef90_E5WJB7_351_584
UniRef90_F6CIV3_222_456
UniRef90_F6DKA0_218_449
UniRef90_E3Z246_18_252
UniRef90_B5YHI6_153_383
UniRef90_A9GF59_268_496
UniRef90_E8WRA5_348_584
UniRef90_Q097K6_265_506
UniRef90_E1KHP7_365_592
UniRef90_A9AVU3_644_869
UniRef90_A6UWZ1_410_640
UniRef90_D4Y401_348_580
UniRef90_D7ATL0_341_566
UniRef90_Q1PXZ9_292_526
UniRef90_E7M6U2_368_603
UniRef90_D7BCF8_586_818
UniRef90_D0MGH9_109_352
UniRef90_UPI000212A698_523_767
UniRef90_E1K386_410_648
UniRef90_B9M7U2_251_475
UniRef90_Q3AAG9_206_440
UniRef90_UPI0001E8932B_350_584
UniRef90_C4G960_243_473
UniRef90_C6J6K9_342_579
UniRef90_A0YQV3_1128_1360

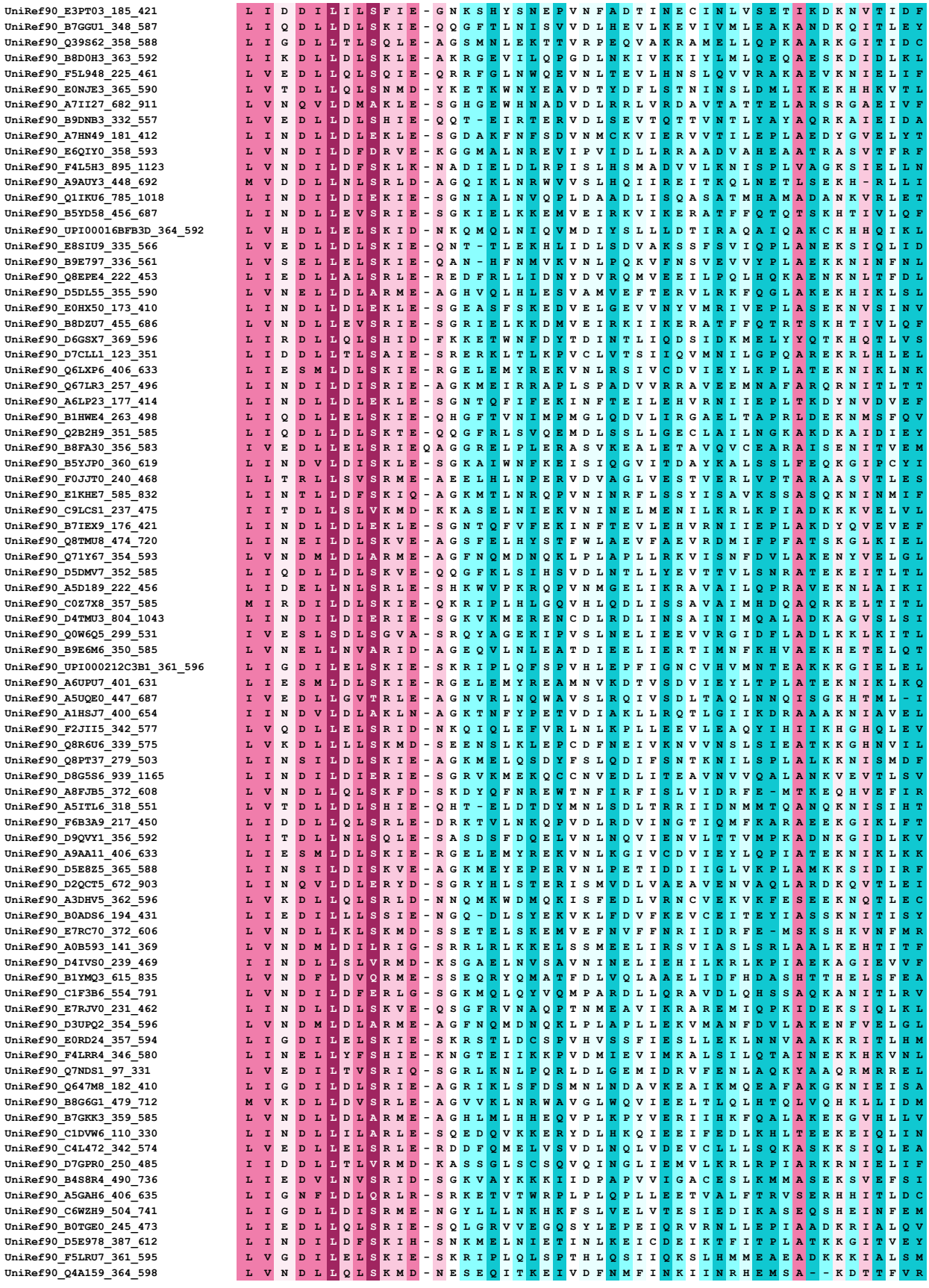
UniRef90_E3PT03_185_421
UniRef90_B7GGU1_348_587
UniRef90_Q39S62_358_588
UniRef90_B8D0H3_363_592
UniRef90_F5L948_225_461
UniRef90_E0NJE3_365_590
UniRef90_A7II27_682_911
UniRef90_B9DNB3_332_557
UniRef90_A7HN49_181_412
UniRef90_E6QIY0_358_593
UniRef90_F4L5H3_895_1123
UniRef90_A9AUY3_448_692
UniRef90_Q1IKU6_785_1018
UniRef90_B5YD58_456_687
UniRef90_UPI00016BFB3D_364_592
UniRef90_E8SIU9_335_566
UniRef90_B9E797_336_561
UniRef90_Q8EPE4_222_453
UniRef90_D5DL55_355_590
UniRef90_E0HX50_173_410
UniRef90_B8DZU7_455_686
UniRef90_D6GSX7_369_596
UniRef90_D7CLL1_123_351
UniRef90_Q6LXP6_406_633
UniRef90_Q67LR3_257_496
UniRef90_A6LP23_177_414
UniRef90_B1HWE4_263_498
UniRef90_Q2B2H9_351_585
UniRef90_B8FA30_356_583
UniRef90_B5YJP0_360_619
UniRef90_F0JJT0_240_468
UniRef90_E1KHE7_585_832
UniRef90_C9LCS1_237_475
UniRef90_B7IEX9_176_421
UniRef90_Q8TMU8_474_720
UniRef90_Q71Y67_354_593
UniRef90_D5DMV7_352_585
UniRef90_A5D189_222_456
UniRef90_C0Z7X8_357_585
UniRef90_D4TMU3_804_1043
UniRef90_Q0W6Q5_299_531
UniRef90_B9E6M6_350_585
UniRef90_UPI000212C3B1_361_596
UniRef90_A6UPU7_401_631
UniRef90_A5UQE0_447_687
UniRef90_A1HSJ7_400_654
UniRef90_F2JII5_342_577
UniRef90_Q8R6U6_339_575
UniRef90_Q8PT37_279_503
UniRef90_D8G5S6_939_1165
UniRef90_A8FJB5_372_608
UniRef90_A5ITL6_318_551
UniRef90_F6B3A9_217_450
UniRef90_D9QVY1_356_592
UniRef90_A9AA11_406_633
UniRef90_D5E8Z5_365_588
UniRef90_D2QCT5_672_903
UniRef90_A3DHV5_362_596
UniRef90_B0ADS6_194_431
UniRef90_E7RC70_372_606
UniRef90_A0B593_141_369
UniRef90_D4IVS0_239_469
UniRef90_B1YMQ3_615_835
UniRef90_C1F3B6_554_791
UniRef90_E7RJV0_231_462
UniRef90_D3UPQ2_354_596
UniRef90_E0RD24_357_594
UniRef90_F4LRR4_346_580
UniRef90_Q7NDS1_97_331
UniRef90_Q647M8_182_410
UniRef90_B8G6G1_479_712
UniRef90_B7GKK3_359_585
UniRef90_C1DVW6_110_330
UniRef90_C4L472_342_574
UniRef90_D7GPR0_250_485
UniRef90_B4S8R4_490_736
UniRef90_A5GAH6_406_635
UniRef90_C6WZH9_504_741
UniRef90_B0TGE0_245_473
UniRef90_D5E978_387_612
UniRef90_F5LRU7_361_595
UniRef90_Q4A159_364_598

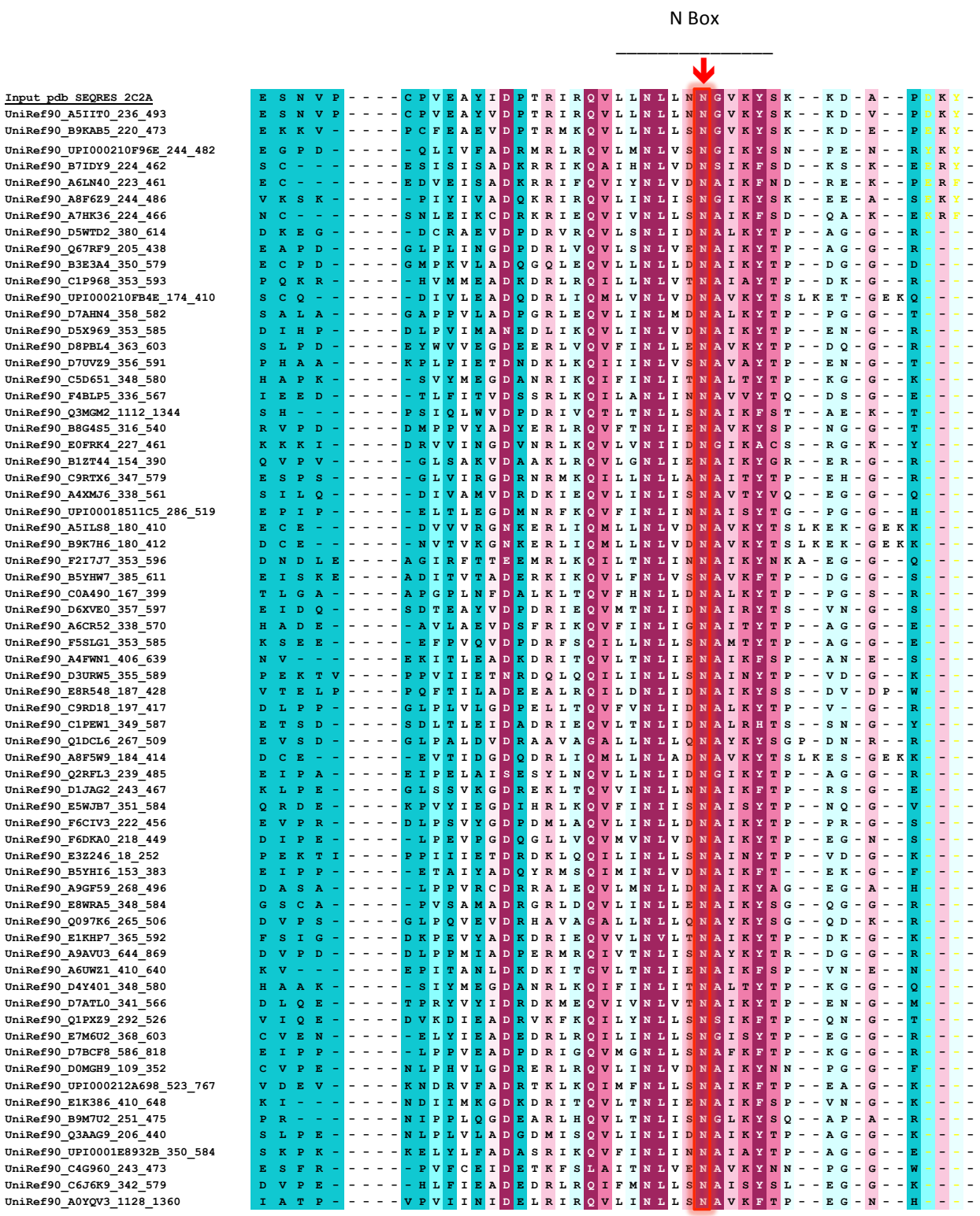
N Box
Input_pdb_SEQRES_2C2A
UniRef90_A5IIT0_236_493
UniRef90_B9KAB5_220_473
UniRef90_UPI000210F96E_244_482
UniRef90_B7IDY9_224_462
UniRef90_A6LN40_223_461
UniRef90_A8F6Z9_244_486
UniRef90_A7HK36_224_466
UniRef90_D5WTD2_380_614
UniRef90_Q67RF9_205_438
UniRef90_B3E3A4_350_579
UniRef90_C1P968_353_593
UniRef90_UPI000210FB4E_174_410
UniRef90_D7AHN4_358_582
UniRef90_D5X969_353_585
UniRef90_D8PBL4_363_603
UniRef90_D7UVZ9_356_591
UniRef90_C5D651_348_580
UniRef90_F4BLP5_336_567
UniRef90_Q3MGM2_1112_1344
UniRef90_B8G4S5_316_540
UniRef90_E0FRK4_227_461
UniRef90_B1ZT44_154_390
UniRef90_C9RTX6_347_579
UniRef90_A4XMJ6_338_561
UniRef90_UPI00018511C5_286_519
UniRef90_A5ILS8_180_410
UniRef90_B9K7H6_180_412
UniRef90_F2I7J7_353_596
UniRef90_B5YHW7_385_611
UniRef90_C0A490_167_399
UniRef90_D6XVE0_357_597
UniRef90_A6CR52_338_570
UniRef90_F5SLG1_353_585
UniRef90_A4FWN1_406_639
UniRef90_D3URW5_355_589
UniRef90_E8R548_187_428
UniRef90_C9RD18_197_417
UniRef90_C1PEW1_349_587
UniRef90_Q1DCL6_267_509
UniRef90_A8F5W9_184_414
UniRef90_Q2RFL3_239_485
UniRef90_D1JAG2_243_467
UniRef90_E5WJB7_351_584
UniRef90_F6CIV3_222_456
UniRef90_F6DKA0_218_449
UniRef90_E3Z246_18_252
UniRef90_B5YHI6_153_383
UniRef90_A9GF59_268_496
UniRef90_E8WRA5_348_584
UniRef90_Q097K6_265_506
UniRef90_E1KHP7_365_592
UniRef90_A9AVU3_644_869
UniRef90_A6UWZ1_410_640
UniRef90_D4Y401_348_580
UniRef90_D7ATL0_341_566
UniRef90_Q1PXZ9_292_526
UniRef90_E7M6U2_368_603
UniRef90_D7BCF8_586_818
UniRef90_D0MGH9_109_352
UniRef90_UPI000212A698_523_767
UniRef90_E1K386_410_648
UniRef90_B9M7U2_251_475
UniRef90_Q3AAG9_206_440
UniRef90_UPI0001E8932B_350_584
UniRef90_C4G960_243_473
UniRef90_C6J6K9_342_579
UniRef90_A0YQV3_1128_1360

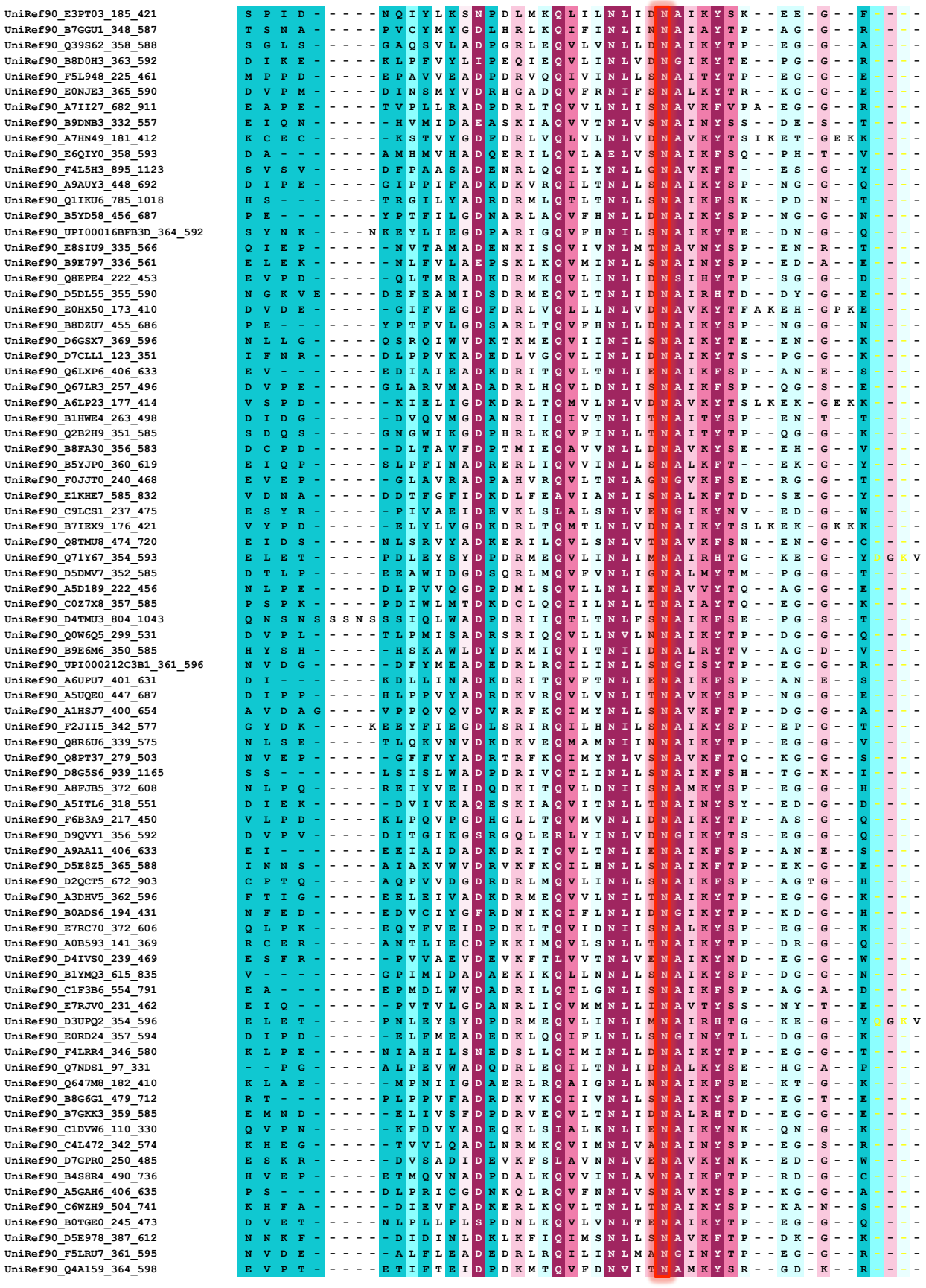
UniRef90_E3PT03_185_421
UniRef90_B7GGU1_348_587
UniRef90_Q39S62_358_588
UniRef90_B8D0H3_363_592
UniRef90_F5L948_225_461
UniRef90_E0NJE3_365_590
UniRef90_A7II27_682_911
UniRef90_B9DNB3_332_557
UniRef90_A7HN49_181_412
UniRef90_E6QIY0_358_593
UniRef90_F4L5H3_895_1123
UniRef90_A9AUY3_448_692
UniRef90_Q1IKU6_785_1018
UniRef90_B5YD58_456_687
UniRef90_UPI00016BFB3D_364_592
UniRef90_E8SIU9_335_566
UniRef90_B9E797_336_561
UniRef90_Q8EPE4_222_453
UniRef90_D5DL55_355_590
UniRef90_E0HX50_173_410
UniRef90_B8DZU7_455_686
UniRef90_D6GSX7_369_596
UniRef90_D7CLL1_123_351
UniRef90_Q6LXP6_406_633
UniRef90_Q67LR3_257_496
UniRef90_A6LP23_177_414
UniRef90_B1HWE4_263_498
UniRef90_Q2B2H9_351_585
UniRef90_B8FA30_356_583
UniRef90_B5YJP0_360_619
UniRef90_F0JJT0_240_468
UniRef90_E1KHE7_585_832
UniRef90_C9LCS1_237_475
UniRef90_B7IEX9_176_421
UniRef90_Q8TMU8_474_720
UniRef90_Q71Y67_354_593
UniRef90_D5DMV7_352_585
UniRef90_A5D189_222_456
UniRef90_C0Z7X8_357_585
UniRef90_D4TMU3_804_1043
UniRef90_Q0W6Q5_299_531
UniRef90_B9E6M6_350_585
UniRef90_UPI000212C3B1_361_596
UniRef90_A6UPU7_401_631
UniRef90_A5UQE0_447_687
UniRef90_A1HSJ7_400_654
UniRef90_F2JII5_342_577
UniRef90_Q8R6U6_339_575
UniRef90_Q8PT37_279_503
UniRef90_D8G5S6_939_1165
UniRef90_A8FJB5_372_608
UniRef90_A5ITL6_318_551
UniRef90_F6B3A9_217_450
UniRef90_D9QVY1_356_592
UniRef90_A9AA11_406_633
UniRef90_D5E8Z5_365_588
UniRef90_D2QCT5_672_903
UniRef90_A3DHV5_362_596
UniRef90_B0ADS6_194_431
UniRef90_E7RC70_372_606
UniRef90_A0B593_141_369
UniRef90_D4IVS0_239_469
UniRef90_B1YMQ3_615_835
UniRef90_C1F3B6_554_791
UniRef90_E7RJV0_231_462
UniRef90_D3UPQ2_354_596
UniRef90_E0RD24_357_594
UniRef90_F4LRR4_346_580
UniRef90_Q7NDS1_97_331
UniRef90_Q647M8_182_410
UniRef90_B8G6G1_479_712
UniRef90_B7GKK3_359_585
UniRef90_C1DVW6_110_330
UniRef90_C4L472_342_574
UniRef90_D7GPR0_250_485
UniRef90_B4S8R4_490_736
UniRef90_A5GAH6_406_635
UniRef90_C6WZH9_504_741
UniRef90_B0TGE0_245_473
UniRef90_D5E978_387_612
UniRef90_F5LRU7_361_595
UniRef90_Q4A159_364_598

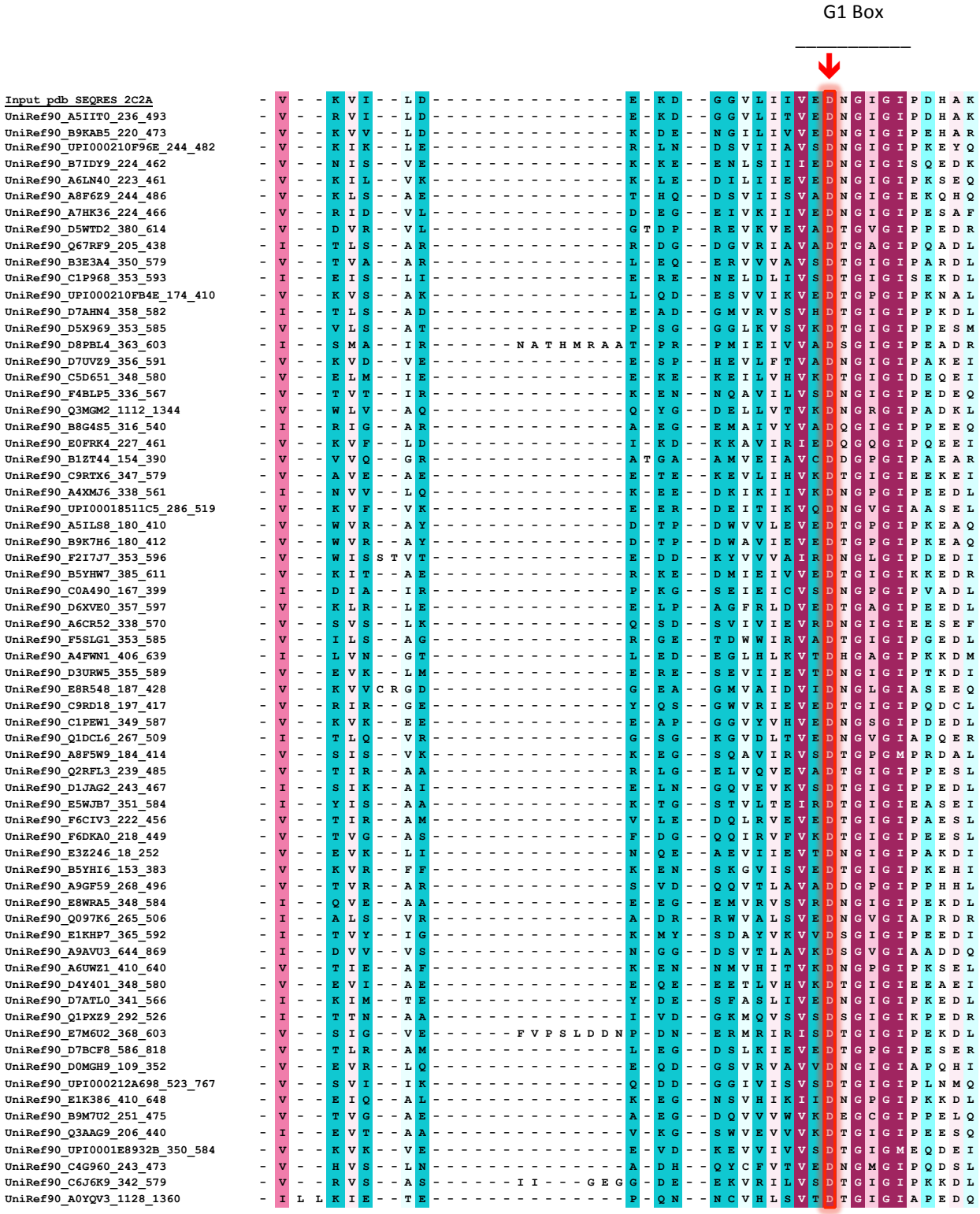
G1 Box
Input pdb SEQRES 2C2A
UniRef90_A5IIT0_236_493
UniRef90_B9KAB5_220_473
UniRef90_UPI000210F96E_244_482
UniRef90_B7IDY9_224_462
UniRef90_A6LN40_223_461
UniRef90_A8F6Z9_244_486
UniRef90_A7HK36_224_466
UniRef90_D5WTD2_380_614
UniRef90_Q67RF9_205_438
UniRef90_B3E3A4_350_579
UniRef90_C1P968_353_593
UniRef90_UPI000210FB4E_174_410
UniRef90_D7AHN4_358_582
UniRef90_D5X969_353_585
UniRef90_D8PBL4_363_603
UniRef90_D7UVZ9_356_591
UniRef90_C5D651_348_580
UniRef90_F4BLP5_336_567
UniRef90_Q3MGM2_1112_1344
UniRef90_B8G4S5_316_540
UniRef90_E0FRK4_227_461
UniRef90_B1ZT44_154_390
UniRef90_C9RTX6_347_579
UniRef90_A4XMJ6_338_561
UniRef90_UPI00018511C5_286_519
UniRef90_A5ILS8_180_410
UniRef90_B9K7H6_180_412
UniRef90_F2I7J7_353_596
UniRef90_B5YHW7_385_611
UniRef90_C0A490_167_399
UniRef90_D6XVE0_357_597
UniRef90_A6CR52_338_570
UniRef90_F5SLG1_353_585
UniRef90_A4FWN1_406_639
UniRef90_D3URW5_355_589
UniRef90_E8R548_187_428
UniRef90_C9RD18_197_417
UniRef90_C1PEW1_349_587
UniRef90_Q1DCL6_267_509
UniRef90_A8F5W9_184_414
UniRef90_Q2RFL3_239_485
UniRef90_D1JAG2_243_467
UniRef90_E5WJB7_351_584
UniRef90_F6CIV3_222_456
UniRef90_F6DKA0_218_449
UniRef90_E3Z246_18_252
UniRef90_B5YHI6_153_383
UniRef90_A9GF59_268_496
UniRef90_E8WRA5_348_584
UniRef90_Q097K6_265_506
UniRef90_E1KHP7_365_592
UniRef90_A9AVU3_644_869
UniRef90_A6UWZ1_410_640
UniRef90_D4Y401_348_580
UniRef90_D7ATL0_341_566
UniRef90_Q1PXZ9_292_526
UniRef90_E7M6U2_368_603
UniRef90_D7BCF8_586_818
UniRef90_D0MGH9_109_352
UniRef90_UPI000212A698_523_767
UniRef90_E1K386_410_648
UniRef90_B9M7U2_251_475
UniRef90_Q3AAG9_206_440
UniRef90_UPI0001E8932B_350_584
UniRef90_C4G960_243_473
UniRef90_C6J6K9_342_579
UniRef90_A0YQV3_1128_1360

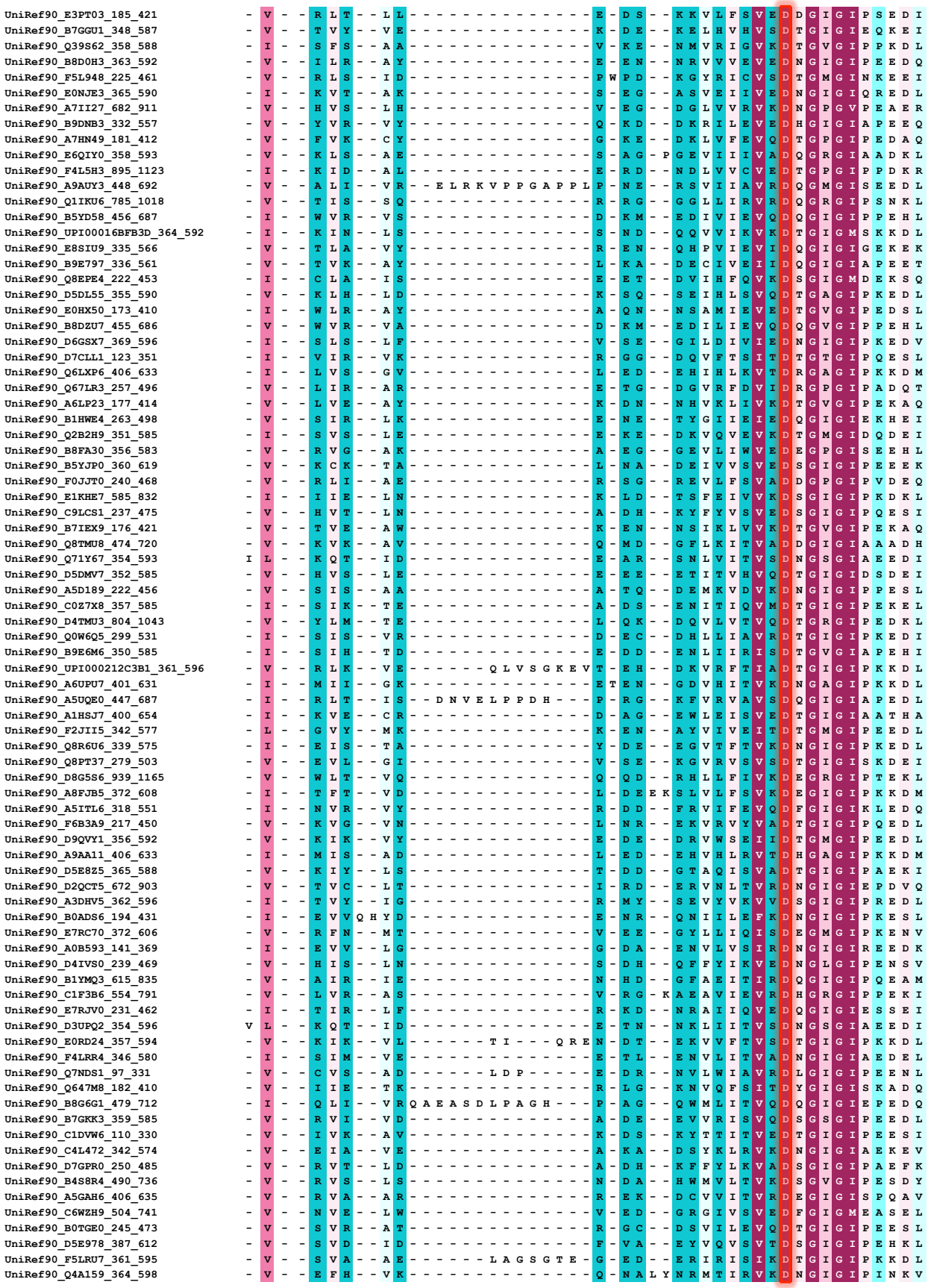
UniRef90_E3PT03_185_421
UniRef90_B7GGU1_348_587
UniRef90_Q39S62_358_588
UniRef90_B8D0H3_363_592
UniRef90_F5L948_225_461
UniRef90_E0NJE3_365_590
UniRef90_A7II27_682_911
UniRef90_B9DNB3_332_557
UniRef90_A7HN49_181_412
UniRef90_E6QIY0_358_593
UniRef90_F4L5H3_895_1123
UniRef90_A9AUY3_448_692
UniRef90_Q1IKU6_785_1018
UniRef90_B5YD58_456_687
UniRef90_UPI00016BFB3D_364_592
UniRef90_E8SIU9_335_566
UniRef90_B9E797_336_561
UniRef90_Q8EPE4_222_453
UniRef90_D5DL55_355_590
UniRef90_E0HX50_173_410
UniRef90_B8DZU7_455_686
UniRef90_D6GSX7_369_596
UniRef90_D7CLL1_123_351
UniRef90_Q6LXP6_406_633
UniRef90_Q67LR3_257_496
UniRef90_A6LP23_177_414
UniRef90_B1HWE4_263_498
UniRef90_Q2B2H9_351_585
UniRef90_B8FA30_356_583
UniRef90_B5YJP0_360_619
UniRef90_F0JJT0_240_468
UniRef90_E1KHE7_585_832
UniRef90_C9LCS1_237_475
UniRef90_B7IEX9_176_421
UniRef90_Q8TMU8_474_720
UniRef90_Q71Y67_354_593
UniRef90_D5DMV7_352_585
UniRef90_A5D189_222_456
UniRef90_C0Z7X8_357_585
UniRef90_D4TMU3_804_1043
UniRef90_Q0W6Q5_299_531
UniRef90_B9E6M6_350_585
UniRef90_UPI000212C3B1_361_596
UniRef90_A6UPU7_401_631
UniRef90_A5UQE0_447_687
UniRef90_A1HSJ7_400_654
UniRef90_F2JII5_342_577
UniRef90_Q8R6U6_339_575
UniRef90_Q8PT37_279_503
UniRef90_D8G5S6_939_1165
UniRef90_A8FJB5_372_608
UniRef90_A5ITL6_318_551
UniRef90_F6B3A9_217_450
UniRef90_D9QVY1_356_592
UniRef90_A9AA11_406_633
UniRef90_D5E8Z5_365_588
UniRef90_D2QCT5_672_903
UniRef90_A3DHV5_362_596
UniRef90_B0ADS6_194_431
UniRef90_E7RC70_372_606
UniRef90_A0B593_141_369
UniRef90_D4IVS0_239_469
UniRef90_B1YMQ3_615_835
UniRef90_C1F3B6_554_791
UniRef90_E7RJV0_231_462
UniRef90_D3UPQ2_354_596
UniRef90_E0RD24_357_594
UniRef90_F4LRR4_346_580
UniRef90_Q7NDS1_97_331
UniRef90_Q647M8_182_410
UniRef90_B8G6G1_479_712
UniRef90_B7GKK3_359_585
UniRef90_C1DVW6_110_330
UniRef90_C4L472_342_574
UniRef90_D7GPR0_250_485
UniRef90_B4S8R4_490_736
UniRef90_A5GAH6_406_635
UniRef90_C6WZH9_504_741
UniRef90_B0TGE0_245_473
UniRef90_D5E978_387_612
UniRef90_F5LRU7_361_595
UniRef90_Q4A159_364_598


F Box
G2 Box
G3
Input pdb SEQRES 2C2A
UniRef90_A5IIT0_236_493
UniRef90_B9KAB5_220_473
UniRef90_UPI000210F96E_244_482
UniRef90_B7IDY9_224_462
UniRef90_A6LN40_223_461
UniRef90_A8F6Z9_244_486
UniRef90_A7HK36_224_466
UniRef90_D5WTD2_380_614
UniRef90_Q67RF9_205_438
UniRef90_B3E3A4_350_579
UniRef90_C1P968_353_593
UniRef90_UPI000210FB4E_174_410
UniRef90_D7AHN4_358_582
UniRef90_D5X969_353_585
UniRef90_D8PBL4_363_603
UniRef90_D7UVZ9_356_591
UniRef90_C5D651_348_580
UniRef90_F4BLP5_336_567
UniRef90_Q3MGM2_1112_1344
UniRef90_B8G4S5_316_540
UniRef90_E0FRK4_227_461
UniRef90_B1ZT44_154_390
UniRef90_C9RTX6_347_579
UniRef90_A4XMJ6_338_561
UniRef90_UPI00018511C5_286_519
UniRef90_A5ILS8_180_410
UniRef90_B9K7H6_180_412
UniRef90_F2I7J7_353_596
UniRef90_B5YHW7_385_611
UniRef90_C0A490_167_399
UniRef90_D6XVE0_357_597
UniRef90_A6CR52_338_570
UniRef90_F5SLG1_353_585
UniRef90_A4FWN1_406_639
UniRef90_D3URW5_355_589
UniRef90_E8R548_187_428
UniRef90_C9RD18_197_417
UniRef90_C1PEW1_349_587
UniRef90_Q1DCL6_267_509
UniRef90_A8F5W9_184_414
UniRef90_Q2RFL3_239_485
UniRef90_D1JAG2_243_467
UniRef90_E5WJB7_351_584
UniRef90_F6CIV3_222_456
UniRef90_F6DKA0_218_449
UniRef90_E3Z246_18_252
UniRef90_B5YHI6_153_383
UniRef90_A9GF59_268_496
UniRef90_E8WRA5_348_584
UniRef90_Q097K6_265_506
UniRef90_E1KHP7_365_592
UniRef90_A9AVU3_644_869
UniRef90_A6UWZ1_410_640
UniRef90_D4Y401_348_580
UniRef90_D7ATL0_341_566
UniRef90_Q1PXZ9_292_526
UniRef90_E7M6U2_368_603
UniRef90_D7BCF8_586_818
UniRef90_D0MGH9_109_352
UniRef90_UPI000212A698_523_767
UniRef90_E1K386_410_648
UniRef90_B9M7U2_251_475
UniRef90_Q3AAG9_206_440
UniRef90_UPI0001E8932B_350_584
UniRef90_C4G960_243_473
UniRef90_C6J6K9_342_579
UniRef90_A0YQV3_1128_1360


UniRef90_E3PT03_185_421
UniRef90_B7GGU1_348_587
UniRef90_Q39S62_358_588
UniRef90_B8D0H3_363_592
UniRef90_F5L948_225_461
UniRef90_E0NJE3_365_590
UniRef90_A7II27_682_911
UniRef90_B9DNB3_332_557
UniRef90_A7HN49_181_412
UniRef90_E6QIY0_358_593
UniRef90_F4L5H3_895_1123
UniRef90_A9AUY3_448_692
UniRef90_Q1IKU6_785_1018
UniRef90_B5YD58_456_687
UniRef90_UPI00016BFB3D_364_592
UniRef90_E8SIU9_335_566
UniRef90_B9E797_336_561
UniRef90_Q8EPE4_222_453
UniRef90_D5DL55_355_590
UniRef90_E0HX50_173_410
UniRef90_B8DZU7_455_686
UniRef90_D6GSX7_369_596
UniRef90_D7CLL1_123_351
UniRef90_Q6LXP6_406_633
UniRef90_Q67LR3_257_496
UniRef90_A6LP23_177_414
UniRef90_B1HWE4_263_498
UniRef90_Q2B2H9_351_585
UniRef90_B8FA30_356_583
UniRef90_B5YJP0_360_619
UniRef90_F0JJT0_240_468
UniRef90_E1KHE7_585_832
UniRef90_C9LCS1_237_475
UniRef90_B7IEX9_176_421
UniRef90_Q8TMU8_474_720
UniRef90_Q71Y67_354_593
UniRef90_D5DMV7_352_585
UniRef90_A5D189_222_456
UniRef90_C0Z7X8_357_585
UniRef90_D4TMU3_804_1043
UniRef90_Q0W6Q5_299_531
UniRef90_B9E6M6_350_585
UniRef90_UPI000212C3B1_361_596
UniRef90_A6UPU7_401_631
UniRef90_A5UQE0_447_687
UniRef90_A1HSJ7_400_654
UniRef90_F2JII5_342_577
UniRef90_Q8R6U6_339_575
UniRef90_Q8PT37_279_503
UniRef90_D8G5S6_939_1165
UniRef90_A8FJB5_372_608
UniRef90_A5ITL6_318_551
UniRef90_F6B3A9_217_450
UniRef90_D9QVY1_356_592
UniRef90_A9AA11_406_633
UniRef90_D5E8Z5_365_588
UniRef90_D2QCT5_672_903
UniRef90_A3DHV5_362_596
UniRef90_B0ADS6_194_431
UniRef90_E7RC70_372_606
UniRef90_A0B593_141_369
UniRef90_D4IVS0_239_469
UniRef90_B1YMQ3_615_835
UniRef90_C1F3B6_554_791
UniRef90_E7RJV0_231_462
UniRef90_D3UPQ2_354_596
UniRef90_E0RD24_357_594
UniRef90_F4LRR4_346_580
UniRef90_Q7NDS1_97_331
UniRef90_Q647M8_182_410
UniRef90_B8G6G1_479_712
UniRef90_B7GKK3_359_585
UniRef90_C1DVW6_110_330
UniRef90_C4L472_342_574
UniRef90_D7GPR0_250_485
UniRef90_B4S8R4_490_736
UniRef90_A5GAH6_406_635
UniRef90_C6WZH9_504_741
UniRef90_B0TGE0_245_473
UniRef90_D5E978_387_612
UniRef90_F5LRU7_361_595
UniRef90_Q4A159_364_598

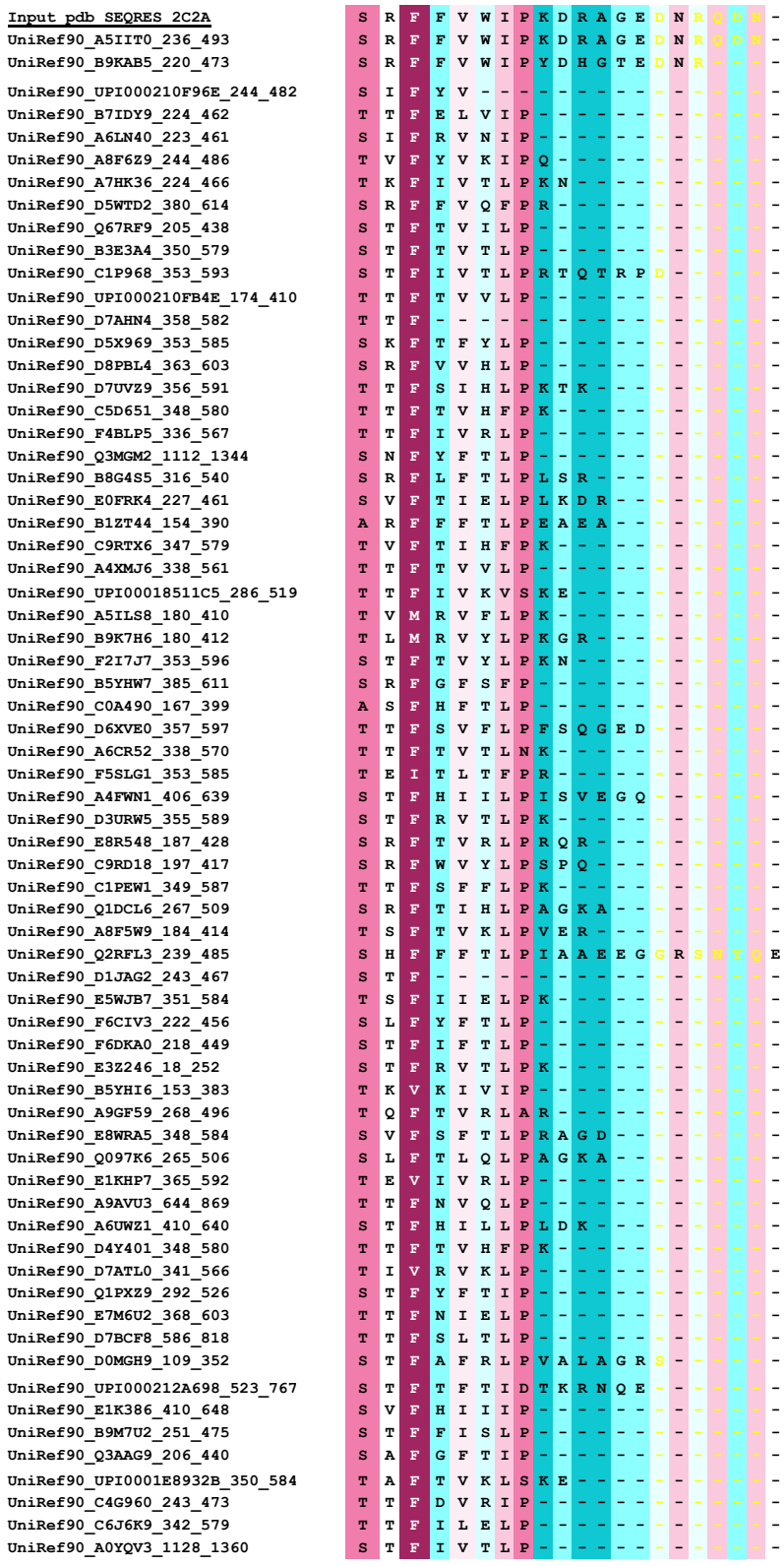
Input pdb SEQRES 2C2A
UniRef90_A5IIT0_236_493
UniRef90_B9KAB5_220_473
UniRef90_UPI000210F96E_244_482
UniRef90_B7IDY9_224_462
UniRef90_A6LN40_223_461
UniRef90_A8F6Z9_244_486
UniRef90_A7HK36_224_466
UniRef90_D5WTD2_380_614
UniRef90_Q67RF9_205_438
UniRef90_B3E3A4_350_579
UniRef90_C1P968_353_593
UniRef90_UPI000210FB4E_174_410
UniRef90_D7AHN4_358_582
UniRef90_D5X969_353_585
UniRef90_D8PBL4_363_603
UniRef90_D7UVZ9_356_591
UniRef90_C5D651_348_580
UniRef90_F4BLP5_336_567
UniRef90_Q3MGM2_1112_1344
UniRef90_B8G4S5_316_540
UniRef90_E0FRK4_227_461
UniRef90_B1ZT44_154_390
UniRef90_C9RTX6_347_579
UniRef90_A4XMJ6_338_561
UniRef90_UPI00018511C5_286_519
UniRef90_A5ILS8_180_410
UniRef90_B9K7H6_180_412
UniRef90_F2I7J7_353_596
UniRef90_B5YHW7_385_611
UniRef90_C0A490_167_399
UniRef90_D6XVE0_357_597
UniRef90_A6CR52_338_570
UniRef90_F5SLG1_353_585
UniRef90_A4FWN1_406_639
UniRef90_D3URW5_355_589
UniRef90_E8R548_187_428
UniRef90_C9RD18_197_417
UniRef90_C1PEW1_349_587
UniRef90_Q1DCL6_267_509
UniRef90_A8F5W9_184_414
UniRef90_Q2RFL3_239_485
UniRef90_D1JAG2_243_467
UniRef90_E5WJB7_351_584
UniRef90_F6CIV3_222_456
UniRef90_F6DKA0_218_449
UniRef90_E3Z246_18_252
UniRef90_B5YHI6_153_383
UniRef90_A9GF59_268_496
UniRef90_E8WRA5_348_584
UniRef90_Q097K6_265_506
UniRef90_E1KHP7_365_592
UniRef90_A9AVU3_644_869
UniRef90_A6UWZ1_410_640
UniRef90_D4Y401_348_580
UniRef90_D7ATL0_341_566
UniRef90_Q1PXZ9_292_526
UniRef90_E7M6U2_368_603
UniRef90_D7BCF8_586_818
UniRef90_D0MGH9_109_352
UniRef90_UPI000212A698_523_767
UniRef90_E1K386_410_648
UniRef90_B9M7U2_251_475
UniRef90_Q3AAG9_206_440
UniRef90_UPI0001E8932B_350_584
UniRef90_C4G960_243_473
UniRef90_C6J6K9_342_579
UniRef90_A0YQV3_1128_1360

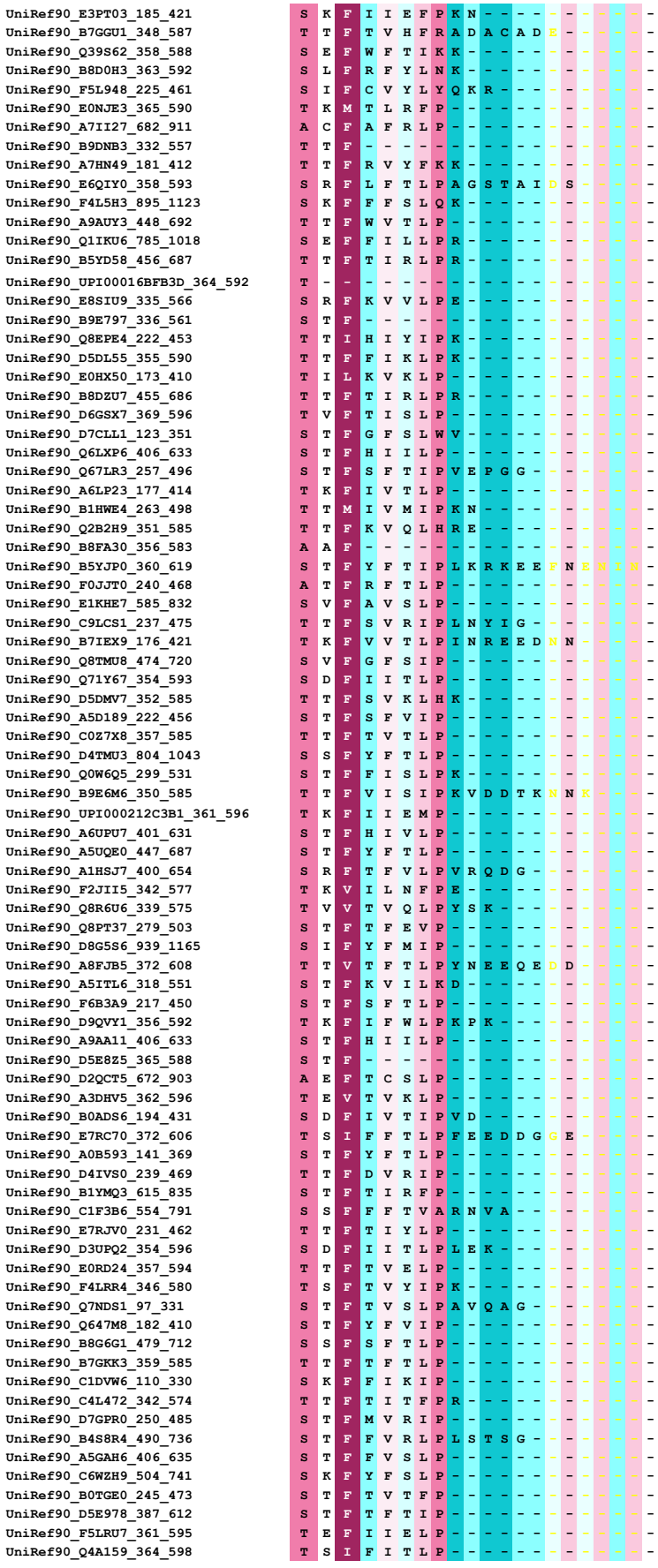
UniRef90_E3PT03_185_421
UniRef90_B7GGU1_348_587
UniRef90_Q39S62_358_588
UniRef90_B8D0H3_363_592
UniRef90_F5L948_225_461
UniRef90_E0NJE3_365_590
UniRef90_A7II27_682_911
UniRef90_B9DNB3_332_557
UniRef90_A7HN49_181_412
UniRef90_E6QIY0_358_593
UniRef90_F4L5H3_895_1123
UniRef90_A9AUY3_448_692
UniRef90_Q1IKU6_785_1018
UniRef90_B5YD58_456_687
UniRef90_UPI00016BFB3D_364_592
UniRef90_E8SIU9_335_566
UniRef90_B9E797_336_561
UniRef90_Q8EPE4_222_453
UniRef90_D5DL55_355_590
UniRef90_E0HX50_173_410
UniRef90_B8DZU7_455_686
UniRef90_D6GSX7_369_596
UniRef90_D7CLL1_123_351
UniRef90_Q6LXP6_406_633
UniRef90_Q67LR3_257_496
UniRef90_A6LP23_177_414
UniRef90_B1HWE4_263_498
UniRef90_Q2B2H9_351_585
UniRef90_B8FA30_356_583
UniRef90_B5YJP0_360_619
UniRef90_F0JJT0_240_468
UniRef90_E1KHE7_585_832
UniRef90_C9LCS1_237_475
UniRef90_B7IEX9_176_421
UniRef90_Q8TMU8_474_720
UniRef90_Q71Y67_354_593
UniRef90_D5DMV7_352_585
UniRef90_A5D189_222_456
UniRef90_C0Z7X8_357_585
UniRef90_D4TMU3_804_1043
UniRef90_Q0W6Q5_299_531
UniRef90_B9E6M6_350_585
UniRef90_UPI000212C3B1_361_596
UniRef90_A6UPU7_401_631
UniRef90_A5UQE0_447_687
UniRef90_A1HSJ7_400_654
UniRef90_F2JII5_342_577
UniRef90_Q8R6U6_339_575
UniRef90_Q8PT37_279_503
UniRef90_D8G5S6_939_1165
UniRef90_A8FJB5_372_608
UniRef90_A5ITL6_318_551
UniRef90_F6B3A9_217_450
UniRef90_D9QVY1_356_592
UniRef90_A9AA11_406_633
UniRef90_D5E8Z5_365_588
UniRef90_D2QCT5_672_903
UniRef90_A3DHV5_362_596
UniRef90_B0ADS6_194_431
UniRef90_E7RC70_372_606
UniRef90_A0B593_141_369
UniRef90_D4IVS0_239_469
UniRef90_B1YMQ3_615_835
UniRef90_C1F3B6_554_791
UniRef90_E7RJV0_231_462
UniRef90_D3UPQ2_354_596
UniRef90_E0RD24_357_594
UniRef90_F4LRR4_346_580
UniRef90_Q7NDS1_97_331
UniRef90_Q647M8_182_410
UniRef90_B8G6G1_479_712
UniRef90_B7GKK3_359_585
UniRef90_C1DVW6_110_330
UniRef90_C4L472_342_574
UniRef90_D7GPR0_250_485
UniRef90_B4S8R4_490_736
UniRef90_A5GAH6_406_635
UniRef90_C6WZH9_504_741
UniRef90_B0TGE0_245_473
UniRef90_D5E978_387_612
UniRef90_F5LRU7_361_595
UniRef90_Q4A159_364_598

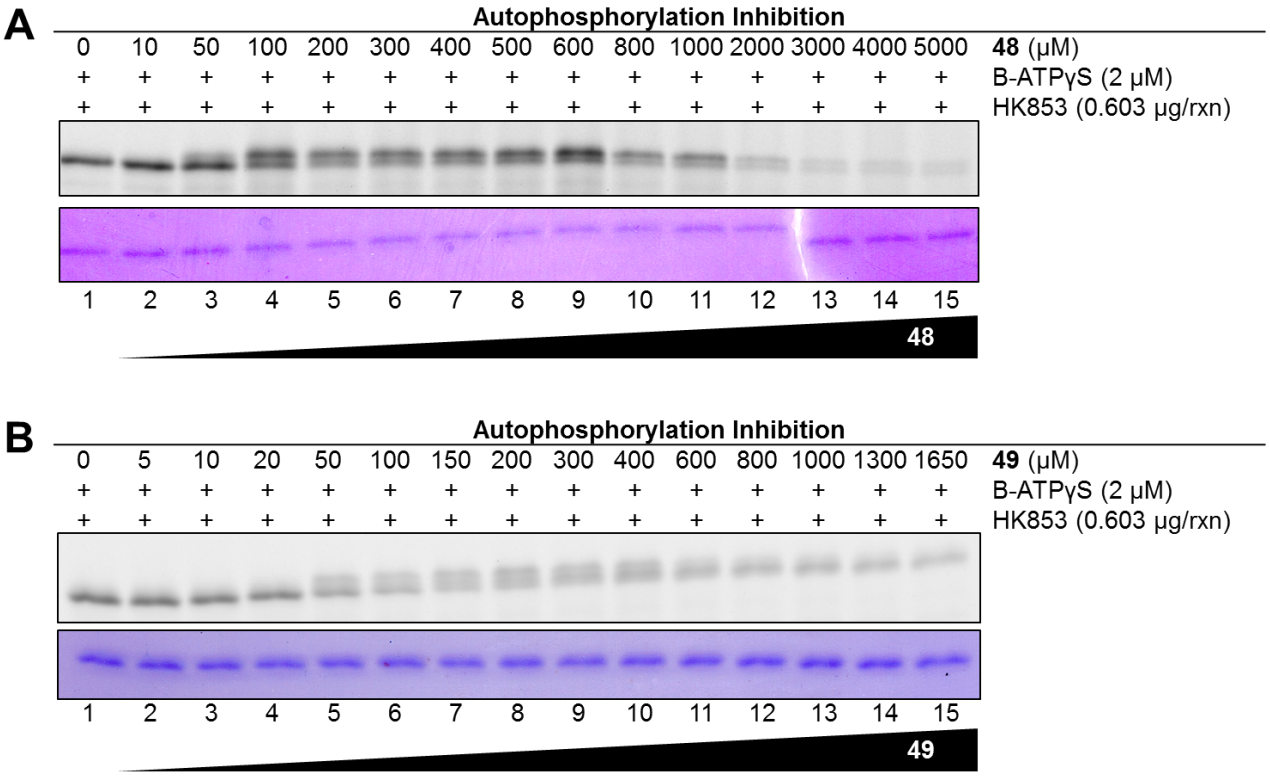

Fig. S6 Competition of HK853 activity in the presence of guanidine derivatives **48** and **49**. Each lane contains 90 ng HK853 (A) Increasing concentrations of **48** competed with B-ATPγS only at concentrations greater than 800 μM (B) Increasing concentrations of **49** competed steadily with B-ATPγS.

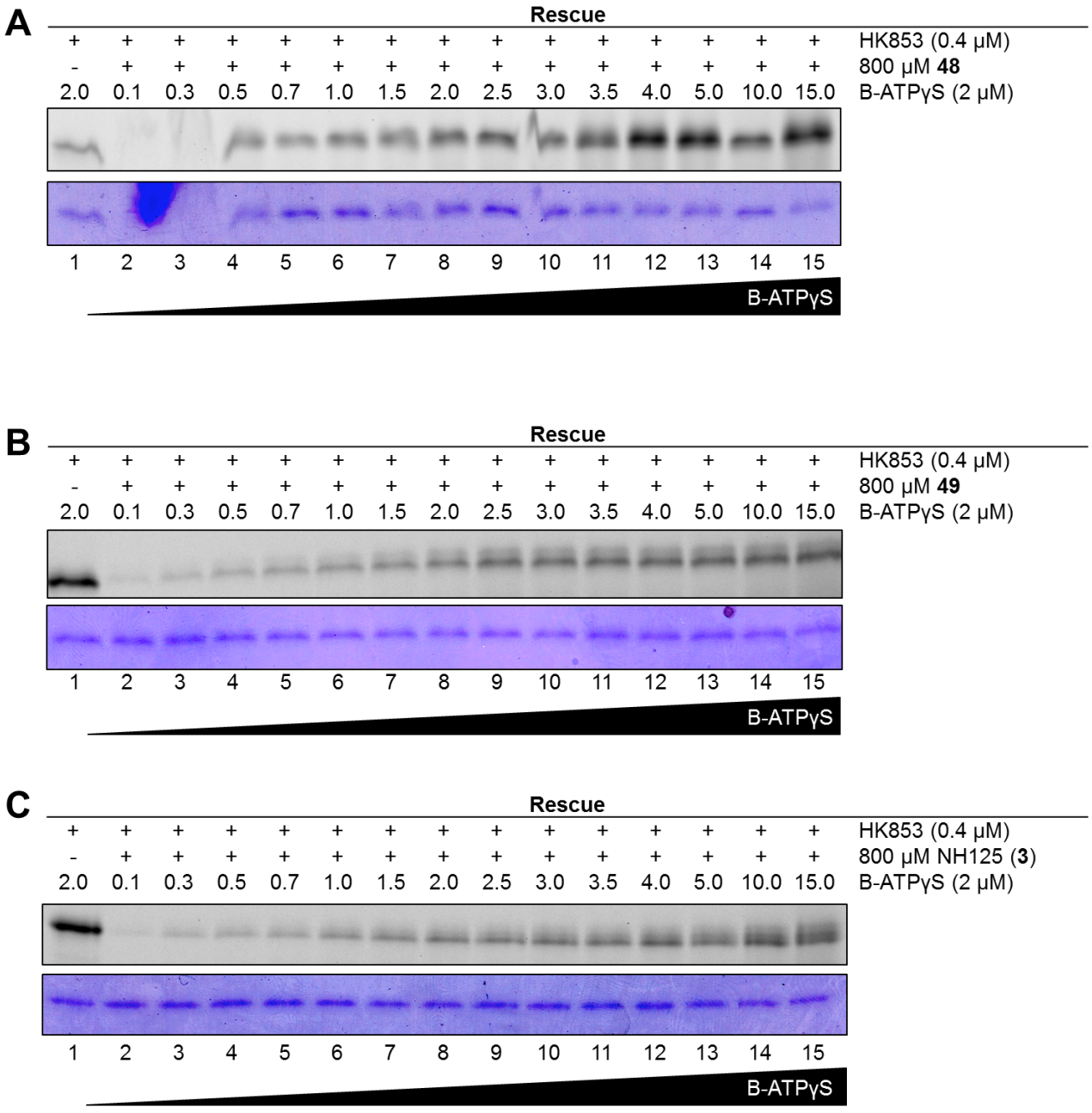

Fig. S7 Rescue of HK853 activity in the presence of inhibitory concentrations of compounds **3**, **48** and **49**. Each lane contains 97 ng HK853. (A) A constant concentration of compound **48** (800 μM) does not show competitive effects on B-ATPγS activity-based labeling of HK853. The defects in lanes 2-4 are due to a deformity in the gel (B) A constant concentration of compound **49** (800 μM) prevents approximately 60% B-ATPγS labeling of HK853. The difference between lanes 1 and 8 illustrates the effects of **49** on the ability of HK853 to autothiophosphorylate. (C) NH125 (**3**) is marketed as an HK inhibitor, and inhibition of HK autophosphorylation was shown in previous studies[19]. A constant concentration of NH125 (**3**) (800 μM) prevents approximately 60% B-ATPγS labeling of HK853. The difference between lanes 1 and 8 illustrates the effects of NH125 (**3**) on the ability of HK853 to autothiophosphorylate.

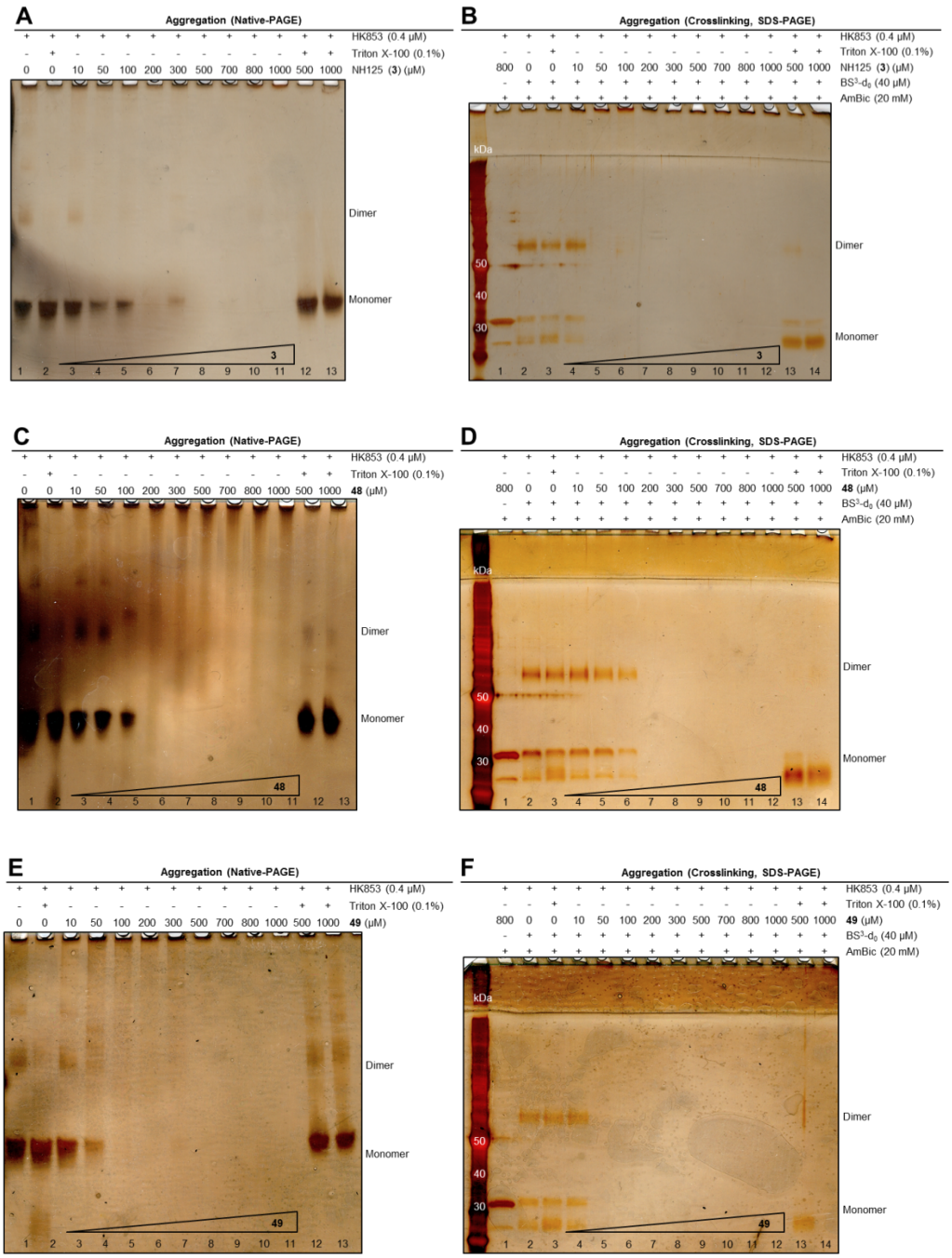

Fig. S8 Aggregation analysis of HK853 in the presence of compounds **3**, **48** and **49**. (A) Native-PAGE shows that HK853 aggregates in the presence of greater than 100 μM of compound **48**. 95 ng of HK853 was loaded in each lane. (B) Crosslinking experiments also show **48** causes aggregation at concentrations greater than 100 μM. 85 ng HK853 was loaded per lane. The addition of Triton X-100 prevents **48**-induced aggregation (C) Native-PAGE shows that HK853 aggregates in the presence ~50 μM **49**. 95 ng of HK853 was loaded in each lane. (D) Crosslinking experiments also show that **49** causes aggregation at concentrations of approximately 50 μM. 85 ng HK853 was loaded per lane. The addition of Triton X-100 prevents **49**-induced aggregation. (E) Native-PAGE shows that HK853 aggregates in the presence of 50-

100 μM NH125 (**3**). 95 ng of HK853 was loaded in each lane. The addition of Triton X-100 prevents NH125 (**3**)-induced aggregation (F) Crosslinking experiments also show that NH125 (**3**) causes aggregation at concentrations greater than 10 μM. 85 ng HK853 was loaded per lane. The addition of Triton X-100 prevents NH125 (**3**)-induced aggregation.

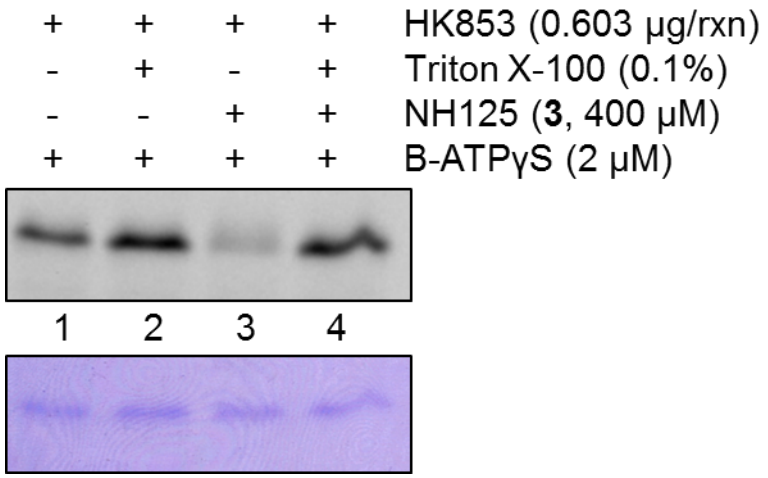

Fig. S9 Triton X-100 restoration of HK853 activity labeling. Since NH125 (**3**) was proposed to be a nonspecific colloidal aggregator[20], Triton X-100 was added to prevent NH 125-induced aggregation. As judged by coomassie staining, there is even loading of protein in lanes 3 and 4. Lane 3 in the fluorescence gel shows a drastic decrease in activity-based labeling; however, restoration of labeling was demonstrated when detergent was added in lane 4. This supports that the mechanism of HK inhibition by NH125 (**3**) is through aggregation. Additionally, Triton X-100 was used in aggregation experiments to restore HK853 to native oligomeric states. 90 ng HK853 was loaded per lane.

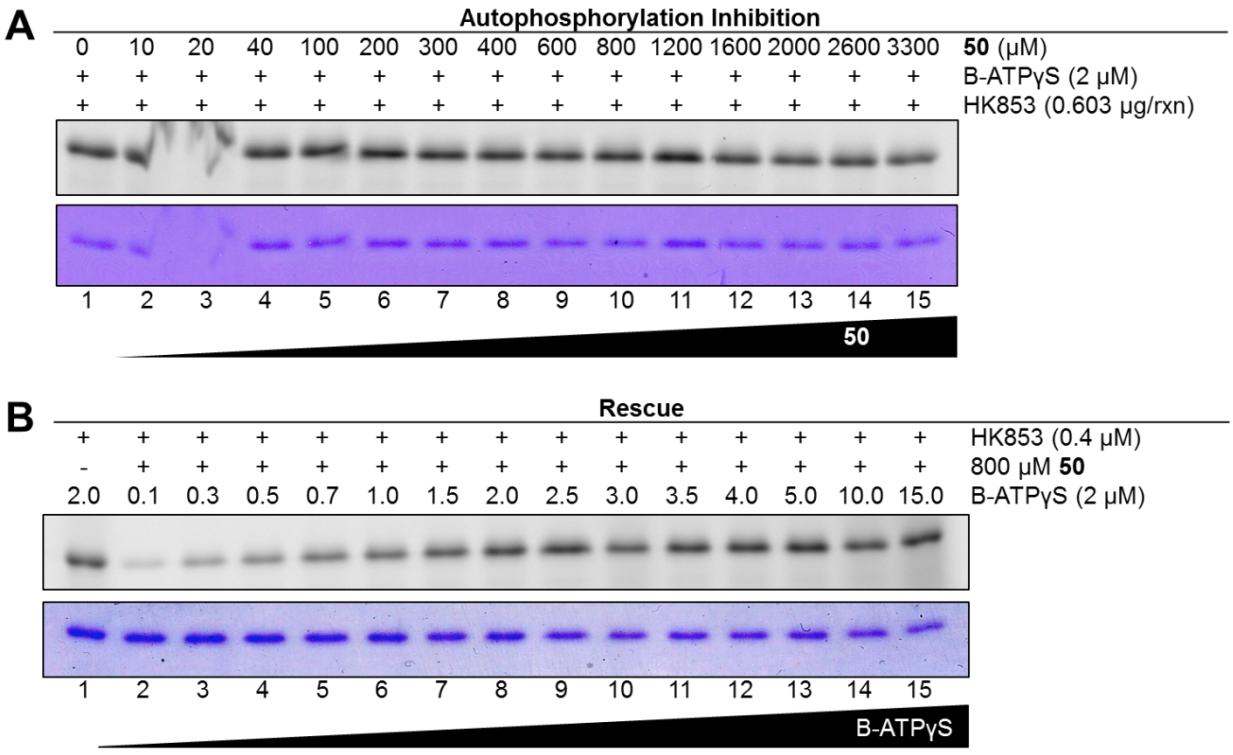

Fig. S10 Competition and rescue of HK853 activity in the presence of compound **50** (A) Increasing concentrations of fragment **50** did not show competition with B-ATPγS. Each lane contains 90 ng HK853. The irregular band shapes in lanes 2 and 3 are due to a deformity in the gel. (B) A constant concentration of fragment **50** (800 μM) has no effect on B-ATPγS activity-based labeling of HK853. 97 ng of HK853 was loaded in each lane.

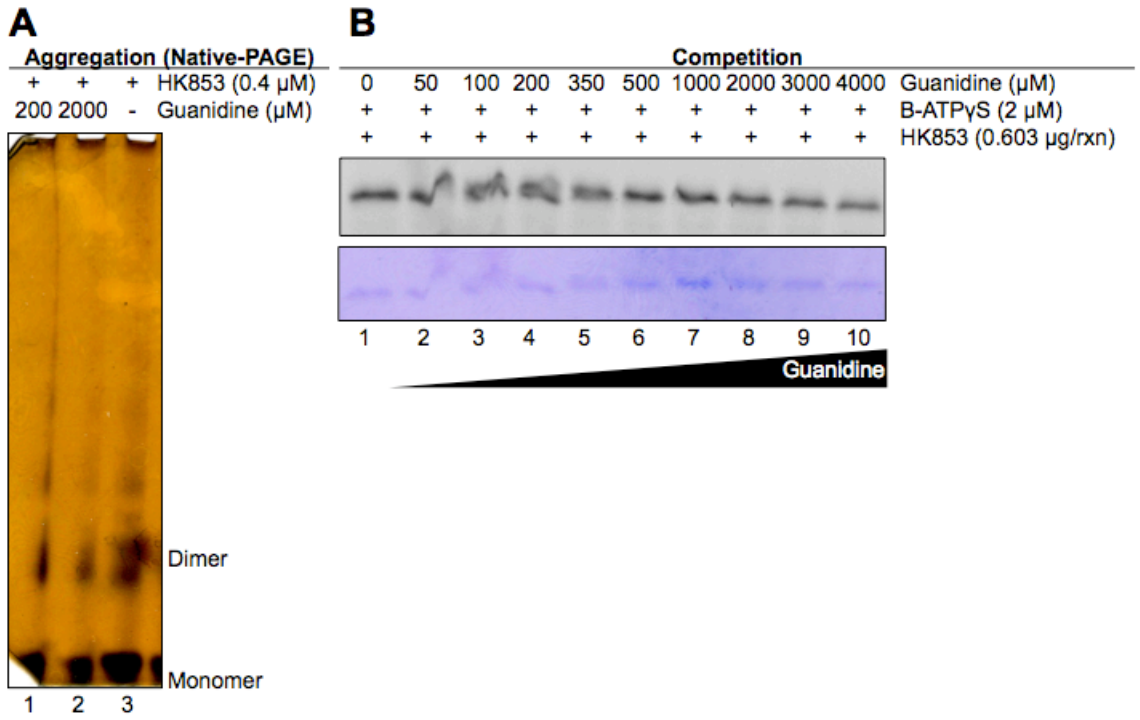

Fig. S11. Analysis of guanidine for HK853 aggregation and competition with activity-based probe. Since guanidinium salts can be used to denature proteins, we wanted to be sure that the guanidine group was not causing denaturation, thus decreasing the activity of HK853. The molar ratio of guanidine:guanidine-HCl is ~0.6:1. Guanidine-HCl was used to prepare known concentrations of guanidine, and the final pH was 8.5. (A) Native-PAGE shows that guanidine does not cause aggregation at concentrations as high as 2 mM. 85 ng HK853 was loaded per lane. (B) Increasing concentrations of guanidine were not shown to affect the autothiophosphorylation of HK853, ensuring that decreases in labeling in activity-based experiments were not due to guanidine-induced denaturation. Each lane contains 90 ng HK853. The irregular band shapes in lanes 2-4 are due to a deformity in the gel.

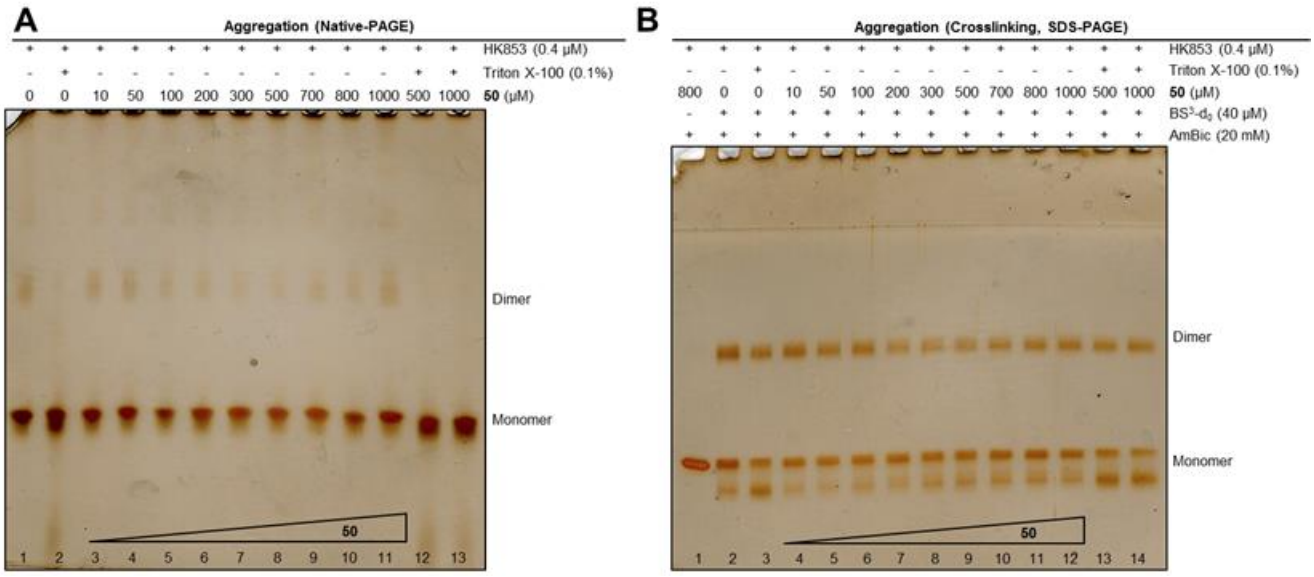

Fig. S12. Aggregation analysis of HK853 in the presence of the fragment **50**. (A) Native-PAGE shows that HK853 does not aggregate in the presence of the fragment **50**. 95 ng of HK853 was loaded in each lane. (B) Crosslinking experiments also show that the fragment **50** does not cause aggregation. 85 ng HK853 was loaded per lane.

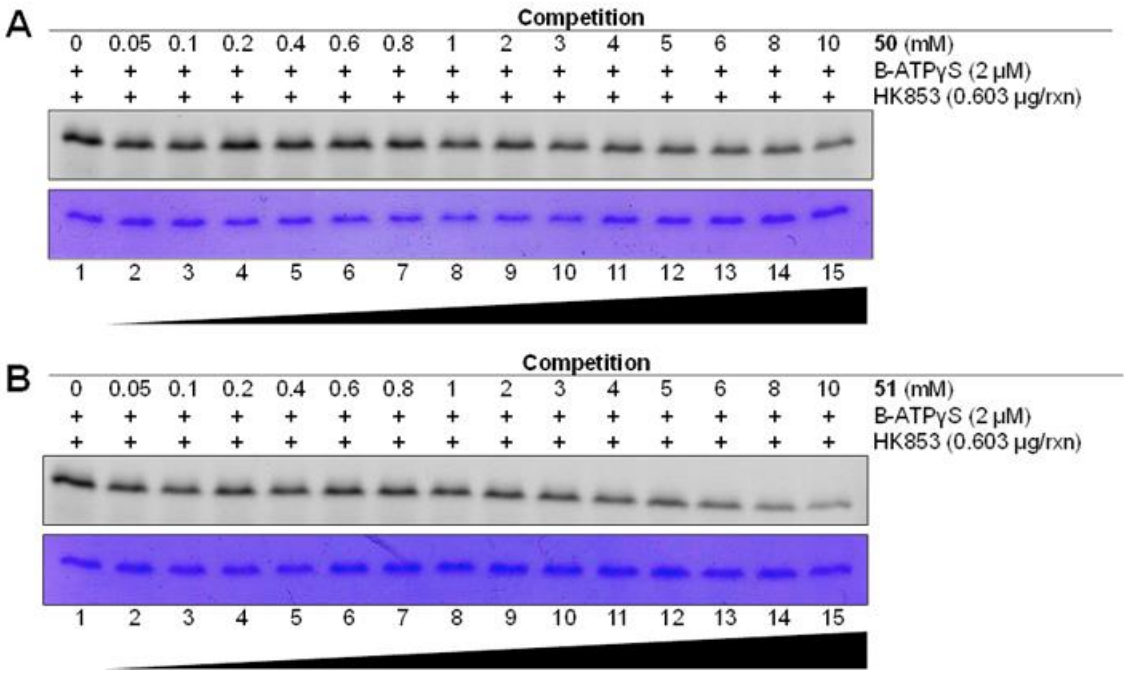

Fig. S13 Competition of HK853 activity in the presence of guanidine fragments **50** and **51**. Each lane contains 90 ng HK853 (A) Increasing concentrations of **50** competed with B-ATPγS (B) Increasing concentrations of **51** competed with B-ATPγS.

Table S2. Competitive ABPP using 2 μM B-ATPγS (probe) and increasing concentrations of **51** (competitor) with HK853. Bands correlate to **Fig. S13 B**.

51 (mM)	Integrated Density of Band Fluorescence (AU)
0.00	271.17
0.05	205.95
0.10	177.52
0.20	216.84
0.40	188.02
0.60	221.99
0.80	212.36
1.00	186.24
2.00	200.62
3.00	188.26
4.00	165.37
5.00	162.81
6.00	139.09
7.00	103.35
10.00	86.01

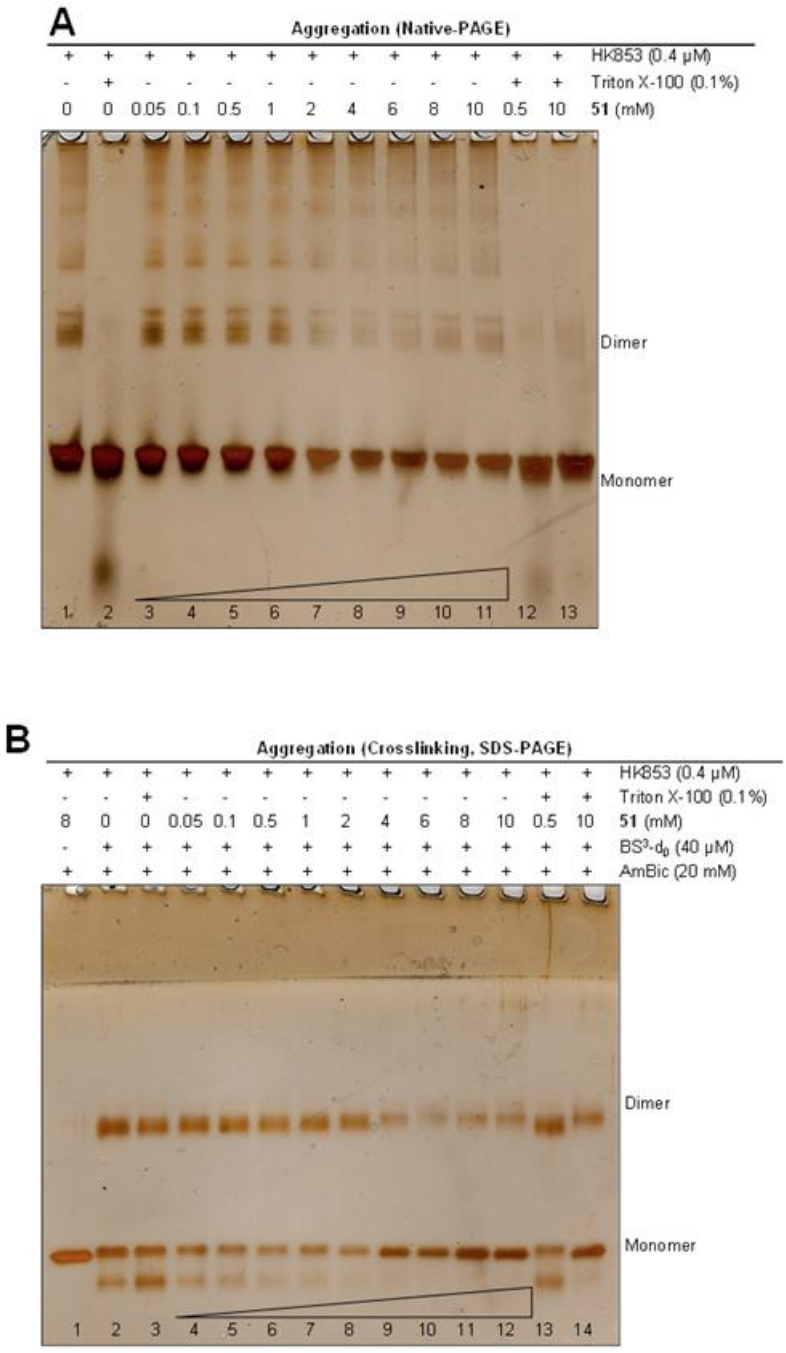

Figure S14. Aggregation analysis of HK853 in the presence of the modified fragment **51**. (A) Native-PAGE shows that HK853 aggregates slightly at concentrations between 4 and 8 mM of **51**. 95 ng of HK853 was loaded in each lane. (B) Crosslinking experiments also show that compound **51** causes subtle aggregation at concentrations in the low micromolar range only. 85 ng HK853 was loaded per lane.

Docking-Based Virtual Screening

General

All molecular modeling operations were performed using SYBYL X2.0 on a quad-core Intel Core i3 workstation operating at 3.06 GHz equipped with 4 GB 1333MHz DDR 3 RAM. Visualization of docked poses was accomplished using the latest available release of UCSF Chimera.

Docking of Compounds.

The active sites of all receptors were defined based on the coordinates of the co-crystallized ligand and the Protomol Generation Mode in Surflex using default settings. A portion of the co-crystallized ligand was retained and used as a guide for the placement of compounds into the active site during docking. The Surflex-Dock parameters were configured as follows:

Max Conformations per Fragment: 10

Max Number of Rotatable Bonds per molecule: 50

Activated: Consider Ring Flexibility

Density of Search: 6.00

Maximum Number of Poses per Ligand: 10

Minimum RMSD Between Final Poses: 0.5

All other parameter were kept at their default values

In Vitro Activity Assays

General Methods and Information

Reagents were obtained from J.T. Baker, Mallinkrodt, Sigma, IBI, VWR, EMD Biosciences, Bio-Rad and Fisher. BODIPY-FL-ATPγS was purchased from Invitrogen, NH125 from Tocris Bioscience, and BS^3-d_0 from Thermo Scientific.

Experimental Methods

HK853 Construct (*Thermotoga maritima*)

The HK853 histidine kinase protein construct was generated as described previously[21]

PCR Site-Directed Mutagenesis for Generation of HK853 D411A Construct[22]

The DNA synthesized for wild-type HK853 was used as a template. Sense and antisense primers that originally coded for D411 were altered to alanine (See Table S3). Primers were ordered from New England Biolabs. Two reactions were prepared in PCR tubes: 2.5 ng HK853 wild-type DNA template, 2.5 µL 2.5 mM dNTPs, 2.5 µL 10 X Pfu buffer, 14.65 µL nuclease-free water, and 0.25 µL 100 X Pfu. To one tube, 2.5 µL of 5 µM mutant sense primer (FHJ088) and 2.5 µL of 5 µM outermost wild-type antisense primer were added. To the other, 2.5 µL of 5 µM outermost wild-type sense primer and 2.5 µL of mutant antisense primer (FHJ089) were added. The final reaction volumes were 25 µL. The PCR reaction was 95°C for 60 s; 30 cycles of 95°C for 30 s, 56°C for 120 s, and 72°C for 90 s; and 72°C for 360 s. To amplify the mutated template, 0.5 µL of product from both the first and second tubes were mixed with 5.0 µL 2.5 mM dNTPs, 5.0 µL of 5 µM outermost sense primer, 5.0 µL of 5 µM outermost antisense primer, 5.0 µL of 10 X Pfu buffer, 28.5 µL nuclease-free water, and 0.5 µL 100 X Pfu to a total volume of 50 µL. The same PCR method was run. PCR product was purified, digested, and ligated into the p-His-parallel vector as before.[23] The DNA sequence was confirmed as successful through sequencing at the Indiana Molecular Biology Institute. Additionally, transformation of p-His-parallel-HK853 D411A

into *E. coli* strain BL21 (DE3)Rosetta, pLysS, and subsequent protein overexpression and purification were performed as described previously[21]. Overexpressed mutant protein is shown in Fig. S15, and the final protein properties are shown in Table S4.

Table S3. Mutant primers used in PCR site-directed mutagenesis to generate HK853 D411A

Primer	Sequence	Comments
KEW026	TGAGAAAGACGGTGGTGTGCTGATCATCGTGGAG**GAT**AATG	Wild-type, sense, Asp
KEW027	GGTCCGGGATGCCGATACCATT**ATC**CTCCACGATGATCAG	Wild-type, antisense, Asp
FHJ088	TGAGAAAGACGGTGGTGTGCTGATCATCGTGGAG**GCG**AATG	Mutant, sense, Ala
FHJ089	GGTCCGGGATGCCGATACCATT**CGC**CTCCACGATGATCAG	Mutant, antisense, Ala

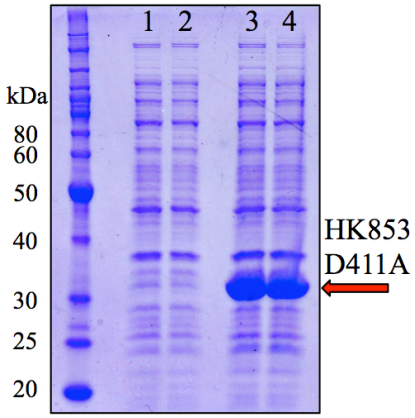

Figure S15. HK853 D411A overexpression. The protein ladder is on the left, non-induced *E. coli* lysate is in lanes 1 and 2 (two separate cultures), and induced *E. coli* lysate is in lanes 3 and 4 (two separate induced cultures).

Table S4. Final protein properties of the HK853 D411A mutant. Gray residues represent a polyhistidine tag coded by the p-His-parallel vector. The red residue is the mutated alanine. Values for pI and extinction coefficient are estimated.

Protein	Sequence	MW (kDa)	pI	ε ($M^{-1}cm^{-1}$)
HK853 D411A	MSYYHHHHHHDYDIPTTENLYFQGAMENVTESKELERLKRIDRMKTEFIANISHELRTPLTAIKA YAETIYNSLGELDLSTLKEFLEVIIDQSNHLENLLNELLDFSRLERKSLQINREKVDLCDLVESAV NAIKEFASSHNVNVLFESNVPCPVEAYIDPTRIRQVLLNLLNNGVKYSKKDAPDKYVKVILDEKD GGVLIIVEANGIGIPDHAKDRIFEQFYRVDSSLTYEVPGTGLGLAITKEIVELHGGRIWVESEVGK GSRFFVWIPKDRAGEDNRQDN	32.4	5.27	27,390

Circular Dichroism (CD) Spectroscopy of HK853 Proteins

Previous CD methods were used as guidelines for this procedure.[24, 25] Using a Jasco J-715 CD spectropolarimeter, CD spectra were acquired for purified HK853 wild-type and D411A proteins. Proteins were exchanged into 10 mM potassium phosphate, pH 7.5, four times using 0.5-mL 10K Amicon Ultra centrifugal filters (Millipore). The Bio-Rad DC Protein Assay was used to determine protein concentrations, which were 0.111 mg/mL for HK853 wild-type and 0.110 mg/mL for HK853 D411A. Buffer and protein solutions were filtered with 0.22-µm Ultrafree-MC centrifugal filters (Millipore) to ensure the removal of any particulates that could interfere with CD readings. Protein solutions were loaded into a 0.1-cm quartz cuvette (Hellma), and spectra were obtained at 25°C. Each spectrum was measured in triplicate with the following parameters: standard (100 mdeg) sensitivity, 190-270 nm range, 0.5 nm data pitch, continuous scanning mode, scanning speed of 100 nm/min, response of 1 s, 1.0-nm bandwidth, and an accumulation of 4 scans. Spectra were smoothed using a Savitsky-Golay filter (15-point smoothing window). Averaged buffer spectra were subtracted from the protein spectra. The CD data in millidegrees were used to calculate mean residue ellipticity, [θ], according to the following equation: [θ]= (millidegrees)/(path length in mm x concentration in M x number of amino acid residues).[25] The final units for mean residue ellipticity were deg cm^{-1} $dmol^{-1}$. Additionally, data from each CD spectrum (in millidegrees) were submitted to Dichroweb for secondary structure analysis using SELCON3 and reference set 4.[26-28] Values for helices, strands, and turns from each spectrum were averaged, and error

was reported as the standard deviation. NRMSD values for Dichroweb results ranged from 0.037 to 0.052.

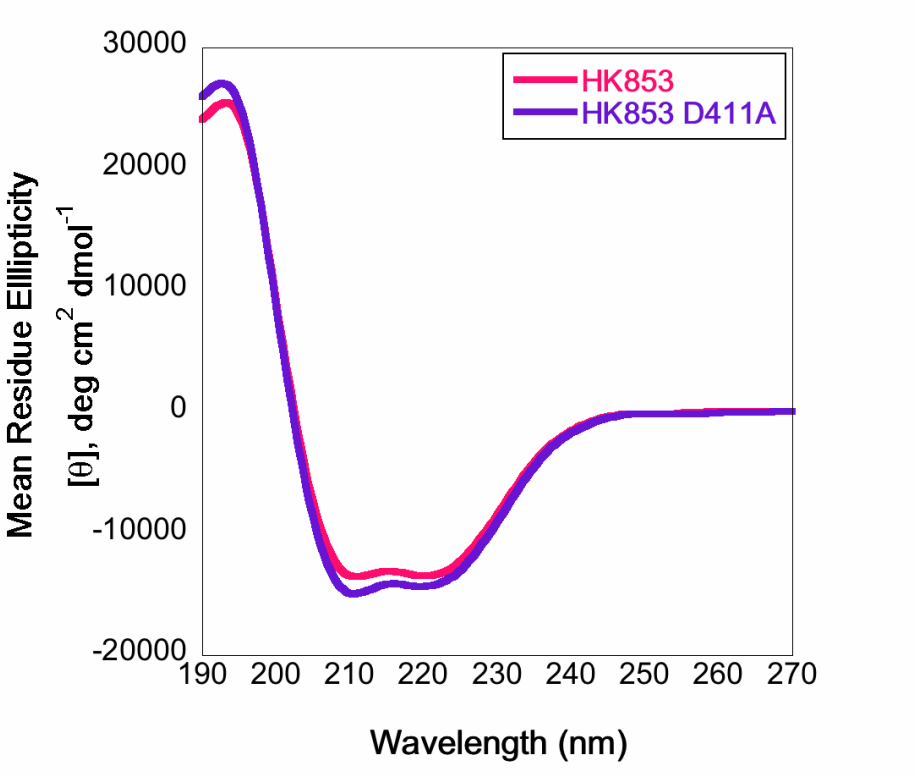

Fig. S16 CD spectra of HK853 wild-type (pink) and D411A (purple) proteins scanned from 190-270 nm shown as mean residue ellipticity.

Table S5 Estimated secondary structure of HK853 proteins (n=3)

Construct	% α-helix	% β-sheet	% turn
HK853 wild-type	42.1 ± 0.3	14.7 ± 0.3	16.6 ± 0.1
HK853 D411A	44.3 ± 0.5	14.1 ± 0.4	16.6 ± 0.3

Rescue ABPP analysis of NH125 (3), 48, 49, 50 and 51

All analogues except AMP-PNP were dissolved in DMSO, and the final DMSO concentration per sample was no greater than 5% (v/v) as stated previously.

Purified HK853 (0.4 μM) in reaction buffer was incubated with a constant concentration (600 or 800 μM) of analogue for 30 min. Individual samples were mixed with 1 μL increasing concentrations of B-ATPγS (0.1-15 μM final concentration) and incubated at RT for 1 h in the dark to prevent fluorophore photobleaching. After incubation, reactions were quenched with 2X SDS-PAGE loading buffer. Samples were not heated before running on SDS-PAGE gels. After analyzing gels by fluorescence, they were coomassie stained.

Saturation Transfer Differential NMR Experiments

All NMR spectra were acquired at 298 K on a Varian DDR 600 MHz spectrometer operating at 599.8 MHz or a Varian DDR 800 MHz spectrometer operating at 799 MHz for 1H, both equipped with a 5mm triple resonance inverse detection probe with z-axis gradient. Saturation transfer difference (STD) spectra were acquired using a standard Varian STD pulse sequence that subtracts NOE spectra from reference spectra during the experiment.[29] Saturation transfer time was 2 s using a 47 ms Gaussian pulse. Irradiation was alternated between 0.73 ppm and 30.2 ppm for the NOE and reference portions, respectively.

Sample preparation

Ligand stocks were made with DMSO-d_6 and phosphate buffers were prepared in D_2O.

Unless otherwise noted, each sample tube contained 5 mM ligand + 0.25 mM protein (20:1 excess of ligand to protein) + 75 mM phosphate buffer in a 500 µL total volume D_2O.

Determination of K_d Using STD-NMR

The approach of Angulo et al. was used to construct the binding isotherms of compounds **50** and **51** to HK853 using the initial growth rates approach (Tables S5 and S6).[11] A variant of the STD-NMR sequence was utilized for selective saturation and the acquisition of on- and-off resonance spectra[30]. Values of 0.73 ppm and 30.2 ppm were used for on- and off resonance frequencies, respectively. To construct the STD buildup curves (Figs. S17 and S18), stock solutions of compounds **50** and **51** in DMSO were titrated (DMSO did not exceed 1% v/v) into a sample of 0.53 µM HK853 in 500 µL D_2O and spectra were acquired at 25 ºC using an array of saturation times of 1, 2, 3 and 4 s. The concentrations of compounds **50** and **51** ranged from 0.6 – 4 mM and the samples were allowed to equilibrate for 15 min between titrations. Plotting the initial slopes and fitting to a Langmuir isotherm yielded the thermodynamic K_d values of **50** and **51**.[31] Data were based on the aromatic protons of **50** (6.80-6.84 ppm) and **51** (7.85-7.90 ppm) and processed using MestreNova 6.02.

Table S5 Initial slopes of the STD build up curves for compound **50**

Ligand concentration (mM)	STD-AF$_{max}$	K$_{sat}$ (s^{-1})	STD-AF$_0$
0.6	184.56	0.68	124.50
0.8	229.83	0.58	132.45
1	307.37	0.44	135.41
2	587.79	0.42	244.66
4	1431	0.23	329.13

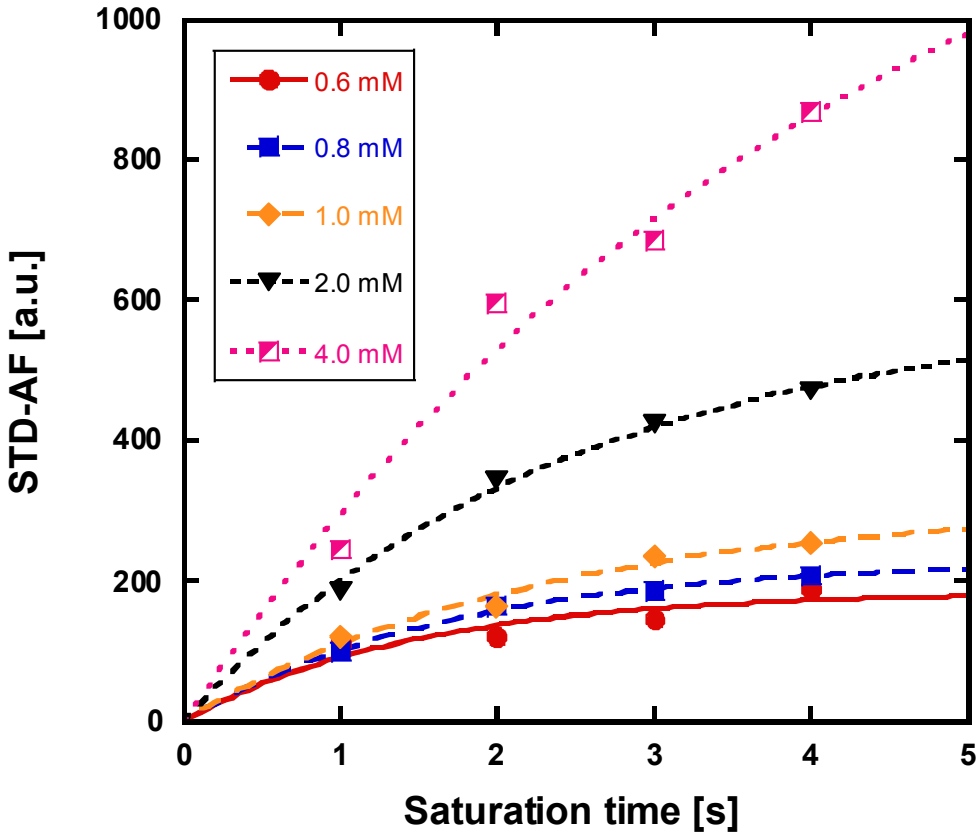

Figure S17. STD-Buildup curves of compound **50**'s binding to HK853.

Table S6 Initial slopes of the STD build up curves for compound **51**

Ligand concentration (mM)	$STD\text{-}AF_{max}$	K_{sat} (s^{-1})	$STD\text{-}AF_0$
0.6	156.17	0.35	53.97
0.8	158.55	0.42	67.25
1	187.77	0.37	69.81
2	327.32	0.25	82.41
3	394.31	0.24	94.37

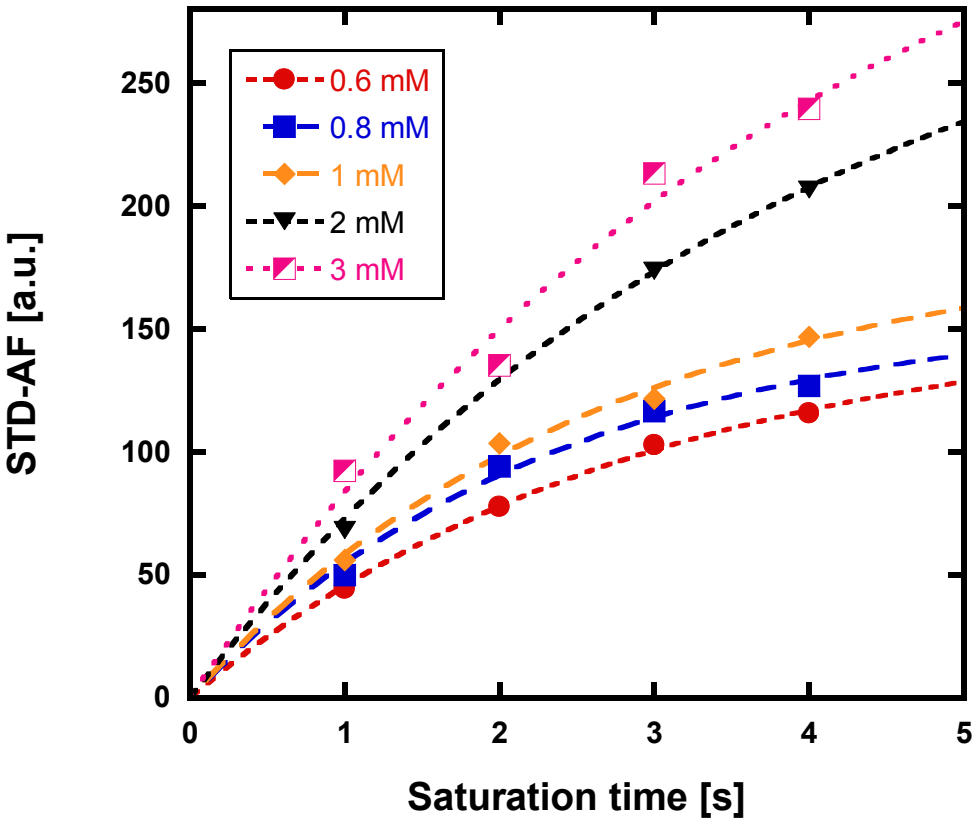

Figure S18. STD-Buildup curves of compound **51**'s binding to HK853.

Measurement of STD Amplification Factors

The STD spectra were quantitatively analyzed by calculation of the STD amplification factors f_{STD}[32] of the averaged aromatic regions of a single sample containing 1 mM tyramine, ADP, **50** and **51** and 0.53 μM HK853 in 500 μL D_2O. Peak processing was performed using VNMRJ.

References

1. S. Roychoudhury, N. A. Zielinski, A. J. Ninfa, N. E. Allen, L. N. Jungheim, T. I. Nicas and A. M. Chakrabarty, *Proc. Natl. Acad. Sci. U. S. A.*, 1993, **90**, 965-969.
2. J. E. Foster, Q. Sheng, J. R. McClain, M. Bures, T. I. Nicas, K. Henry, M. E. Winkler and R. Gilmour, *Microbiology*, 2004, **150**, 885-896.
3. N. Li, F. Wang, S. Niu, J. Cao, K. Wu, Y. Li, N. Yin, X. Zhang, W. Zhu and Y. Yin, *BMC Microbiol.*, 2009, **9**, 129.
4. Z. Qin, J. Zhang, B. Xu, L. Chen, Y. Wu, X. Yang, X. Shen, S. Molin, A. Danchin, H. Jiang and D. Qu, *BMC Microbiol.*, 2006, **6**, 96.
5. R. Gilmour, J. E. Foster, Q. Sheng, J. R. McClain, A. Riley, P.-M. Sun, W.-L. Ng, D. Yan, T. I. Nicas, K. Henry and M. E. Winkler, *J. Bacteriol.*, 2005, **187**, 8196-8200.
6. E. Furuta, K. Yamamoto, D. Tatebe, K. Watabe, T. Kitayama and R. Utsumi, *FEBS Lett.*, 2005, **579**, 2065-2070.
7. J. J. Hilliard, R. M. Goldschmidt, L. Licata, E. Z. Baum and K. Bush, *Antimicrob. Agents Chemother.*, 1999, **43**, 1693-1699.
8. D. J. Hlasta, J. P. Demers, B. D. Foleno, S. A. Fraga-Spano, J. Guan, J. J. Hilliard, M. J. Macielag, K. A. Ohemeng, C. M. Sheppard, Z. Sui, G. C. Webb, M. A. Weidner-Wells, H. Werblood and J. F. Barrett, *Bioorg. Med. Chem. Lett.*, 1998, **8**, 1923-1928.
9. Z. Sui, J. Guan, D. J. Hlasta, M. J. Macielag, B. D. Foleno, R. M. Goldschmidt, M. J. Loeloff, G. C. Webb and J. F. Barrett, *Bioorg. Med. Chem. Lett.*, 1998, **8**, 1929-1934.
10. J. F. Barrett, R. M. Goldschmidt, L. E. Lawrence, B. Foleno, R. Chen, J. P. Demers, S. Johnson, R. Kanojia, J. Fernandez, J. Bernstein, L. Licata, A. Donetz, S. Huang, D. J. Hlasta, M. J. Macielag, K. Ohemeng, R. Frechette, M. B. Frosco, D. H. Klaubert, J. M. Whiteley, L. Wang and J. A. Hoch, *Proc. Natl. Acad. Sci. U. S. A.*, 1998, **95**, 5317-5322.
11. J. Angulo, P. M. Enríquez-Navas and P. M. Nieto, *Chemistry – A European Journal*, 2010, **16**, 7803-7812.
12. R. M. Kanojia, W. Murray, J. Bernstein, J. Fernandez, B. D. Foleno, H. Krause, L. Lawrence, G. Webb and J. F. Barrett, *Bioorg. Med. Chem. Lett.*, 1999, **9**, 2947-2952.
13. H. Ramström, M. Bourotte, C. Philippe, M. Schmitt, J. Haiech and J.-J. Bourguignon, *J. Med. Chem.*, 2004, **47**, 2264-2275.
14. S. J. Trew, S. K. Wrigley, L. Pairet, J. Sohal, P. Shanu-Wilson, M. A. Hayes, S. M. Martin, R. N. Manohar, M. I. Chicarelli-Robinson, D. A. Kau, C. V. Byrne, E. M. Wellington, J. M. Moloney, J. Howard, D. Hupe and E. R. Olson, *J. Antibiot. (Tokyo)*, 2000, **53**, 1-11.
15. A. Okada, Y. Gotoh, T. Watanabe, E. Furuta, K. Yamamoto and R. Utsumi, *Methods Enzymol.*, 2007, **422**, 386-395.
16. T. Kitayama, R. Iwabuchi, S. Minagawa, S. Sawada, R. Okumura, K. Hoshino, J. Cappiello and R. Utsumi, *Bioorg. Med. Chem. Lett.*, 2007, **17**, 1098-1101.

17. Z. Qin, B. Lee, L. Yang, J. Zhang, X. Yang, D. Qu, H. Jiang and S. Molin, *FEMS Microbiol. Lett.*, 2007, **273**, 149-156.
18. H. Ashkenazy, E. Erez, E. Martz, T. Pupko and N. Ben-Tal, *Nucleic Acids Res.*, 2010, **38**, W529-W533.
19. A. M. Bilwes, C. M. Quezada, L. R. Croal, B. R. Crane and M. I. Simon, *Nat. Struct. Mol. Biol.*, 2001, **8**, 353-360.
20. A. Hirschman, M. Boukhvalova, R. VanBruggen, A. J. Wolfe and R. C. Stewart, *Biochemistry*, 2001, **40**, 13876-13887.
21. K. E. Wilke, S. Francis and E. E. Carlson, *J. Am. Chem. Soc.*, 2012, **134**, 9150-9153.
22. K. L. Heckman and L. R. Pease, *Nat. Protocols*, 2007, **2**, 924-932.
23. P. Sheffield, S. Garrard and Z. Derewenda, *Protein Expr. Purif.*, 1999, **15**, 34-39.
24. A. D. Gutu, K. J. Wayne, L.-T. Sham and M. E. Winkler, *J. Bacteriol.*, 2010, **192**, 2346-2358.
25. N. J. Greenfield, *Nat. Protocols*, 2007, **1**, 2876-2890.
26. L. Whitmore and B. A. Wallace, *Biopolymers*, 2008, **89**, 392-400.
27. L. Whitmore and B. A. Wallace, *Nucleic Acids Res.*, 2004, **32**, W668-W673.
28. A. Lobley, L. Whitmore and B. A. Wallace, *Bioinformatics*, 2002, **18**, 211-212.
29. J. Seidler, S. L. McGovern, T. N. Doman and B. K. Shoichet, *J. Med. Chem.*, 2003, **46**, 4477-4486.
30. M. Mayer and B. Meyer, *J. Am. Chem. Soc.*, 2001, **123**, 6108-6117.
31. Due to artifacts in the STD spectra, points at the concentration intervals of 3 mM (**50**) and 4 mM (**51**) were excluded from the plot.
32. S. Barelier, J. Pons, K. Gehring, J.-M. Lancelin and I. Krimm, *J. Med. Chem.*, 2010, **53**, 5256-5266.